

# 1 **Bacterial degradation activity in the Eastern Tropical South**

## 2 **Pacific oxygen minimum zone**

3 Marie Maßmig, Jan Lüdke, Gerd Krahmann, Anja Engel\*

4 GEOMAR Helmholtz Centre for Ocean Research Kiel, Düsternbrooker Weg 20, D-24105 Kiel, Germany

5 *Correspondence to:* Anja Engel (aengel@geomar.de)

6 **Abstract.** Oxygen minimum zones (OMZs) show distinct biogeochemical processes that relate to microorganisms  
7 being able to thrive under low or even absent oxygen. Microbial degradation of organic matter is expected to be reduced  
8 in OMZs, although quantitative evidence is low. Here, we present heterotrophic bacterial production ( $^3\text{H}$  leucine-  
9 incorporation), extracellular enzyme rates (leucine aminopeptidase / $\beta$ -glucosidase) and bacterial cell abundance for  
10 various *in situ* oxygen concentrations in the water column, including the upper and lower oxycline, of the Eastern  
11 Tropical South Pacific off Peru. Bacterial heterotrophic activity in the suboxic core of the OMZ (at *in situ*  $\leq 5 \mu\text{mol O}_2 \text{ kg}^{-1}$ )  
12 ranged from 0.3 to  $281 \mu\text{mol C m}^{-3} \text{ d}^{-1}$  and was not significantly lower than in waters of  $5\text{--}60 \mu\text{mol O}_2 \text{ kg}^{-1}$ .  
13 Moreover, bacterial abundance in the OMZ and leucine aminopeptidase activity were significantly higher in suboxic  
14 waters compared to waters of  $5\text{--}60 \mu\text{mol O}_2 \text{ kg}^{-1}$ , suggesting no impairment of bacterial organic matter degradation in  
15 the core of the OMZ. Nevertheless, high cell-specific bacterial production was observed in samples from oxyclines  
16 and cell-specific extracellular enzyme rates were especially high at the lower oxycline, corroborating earlier findings  
17 of highly active and distinct micro-aerobic bacterial communities. To assess the impact of bacterial degradation of  
18 dissolved organic matter (DOM) for oxygen loss in the Peruvian OMZ, we compared diapycnal fluxes of oxygen and  
19 dissolved organic carbon (DOC) and their microbial uptake within the upper 60m of the water column. Our data  
20 indicate low bacterial growth efficiencies of 1-21% at the upper oxycline, resulting in a high bacterial oxygen demand  
21 that can explain up to 33% of the observed average oxygen loss over depth. Our study therewith shows that microbial  
22 degradation of DOM has a considerable share in sustaining the OMZ off Peru.

23      **1. Introduction**

24      In upwelling zones at eastern continental margins, oxygen minimum zones (OMZs) with hypoxic ( $<60 \mu\text{mol O}_2 \text{ kg}^{-1}$ ),  
25      suboxic ( $<5 \mu\text{mol O}_2 \text{ kg}^{-1}$ ) or even anoxic conditions occur (Gruber, 2011; Thamdrup et al., 2012; Tiano et al., 2014).  
26      OMZs have expanded over the past years resulting in an ~3.7 % increase of hypoxic waters at depth (200 dbar) between  
27      1960 and 2008 (Stramma et al., 2010). One of the largest anoxic water masses in the global ocean ( $2.4 \times 10^{13} \text{ m}^3$ ) is  
28      located in the Eastern Tropical South Pacific and includes the Peruvian upwelling system (Kämpf and Chapman, 2016;  
29      Paulmier and Ruiz-Pino, 2009; Thamdrup et al., 2012). There, nutrient-rich water is upwelled and supports high rates  
30      of primary production and accumulation of organic matter. Biological degradation of organic matter subsequently  
31      reduces oxygen below the surface mixed layer (Kämpf and Chapman, 2016). As a consequence, and supported by  
32      sluggish ventilation of water masses, a permanent OMZ forms between 100 and 500 m depth, with upper and lower  
33      boundaries, i.e. oxyclines, varying within seasonal and inter-annual cycles (Czeschel et al., 2011; Graco et al., 2017;  
34      Kämpf and Chapman, 2016). In austral winter, upwelling and subsequently the nutrient supply to the surface waters  
35      increase (Bakund and Nelson, 1991; Echevin et al., 2008). However, chlorophyll *a* (Chl *a*) concentration is highest in  
36      austral summer, with the seasonal amplitude being stronger for surface than for depth averaged Chl *a* concentrations  
37      (Echevin et al., 2008). In winter, phytoplankton growth is, next to iron, mainly limited by light due to the deeper  
38      mixing, whereas in summer macronutrients can become a limiting factor (Echevin et al., 2008). Further, El Niño–  
39      Southern Oscillation may affect organic matter cycling in the area since it affects the depth of the oxycline and therefore  
40      the extent of anaerobic processes in the upper water column (Llanillo et al., 2013). During the year of this study (2017),  
41      neither a strong La Niña nor a strong El Niño was detected (<https://ggweather.com/enso/oni.htm>). However, in January,  
42      February and March 2017 there was a strong coastal El Niño with enhanced warming (+1.5°C) of sea surface  
43      temperatures in the eastern Pacific (Garreaud, 2018).

44      Within OMZs, enhanced vertical carbon export has been observed (Devol and Hartnett, 2001; Roullier et al., 2014)  
45      and explained by a potentially reduced remineralization of organic matter in suboxic and anoxic waters. This is possibly  
46      because microbes apply anaerobic respiratory pathways that yield less metabolic energy compared to aerobic  
47      respiration. For instance, denitrification or dissimilatory nitrate reduction to ammonia (DNRA) result only in 99 %, or  
48      64 % of the energy (kJ) per oxidized carbon atom that is produced by aerobic respiration (Lam and Kuypers, 2011).  
49      Additionally, the energy yield available for the production of cell mass seems to be less than expected from the  
50      chemical equations (Strohm et al., 2007). Meanwhile, bacteria are mainly responsible for the remineralization of  
51      organic matter into nutrients and carbon dioxide (CO<sub>2</sub>) in the ocean (Azam et al., 1983). Thus, microbial activity and  
52      consequently organic matter remineralization in suboxic and anoxic waters might be reduced, possibly explaining  
53      enhanced export of carbon. As a consequence, expanding OMZs could result in increased CO<sub>2</sub> storage in the ocean.

54      During the degradation process, low molecular weight (LMW <1 kDa) organic compounds can directly be taken up  
55      by bacteria (Azam et al., 1983; Weiss et al., 1991). However, in the ocean, bioavailable organic matter is commonly  
56      in the form of particulate organic matter or high molecular weight (HMW) DOM (Benner and Amon, 2015). To access  
57      this organic matter pool, bacteria produce extracellular, substrate specific enzymes that hydrolyse polymers into LMW  
58      units (Hoppe et al., 2002). Taken-up, organic matter is partly incorporated into bacterial biomass, or respired to CO<sub>2</sub>,

59 which may evade to the atmosphere (Azam et al., 1983). Rates of enzymatic organic matter hydrolysis or bacterial  
60 production are controlled by the environment, i.e. temperature and pH, but can be actively regulated e.g. in response  
61 to changing organic matter supply and quality (Boetius and Lochte, 1996; Grossart et al., 2006; Pantoja et al., 2009;  
62 Piontek et al., 2014). However, the effect of oxygen concentration, which dictates the respiratory pathway and thus  
63 energy gain, on bacterial production and the expression of extracellular enzymes in aquatic systems, is poorly  
64 understood. For instance, bacterial production was higher in anoxic lake waters (Cole and Pace, 1995), whereas in the  
65 Pacific waters off Chile bacterial production and DOM decomposition rates did not change in relation to oxygen  
66 concentrations (Lee, 1992; Pantoja et al., 2009). Investigations of hydrolysis rates as the initial step of organic matter  
67 degradation, may help to unravel possible adaptation strategies of bacterial communities to suboxic and anoxic  
68 conditions (Hoppe et al., 2002). High extracellular enzyme rates might compensate a putative lower energy yield of  
69 anaerobic respiration and the subsequent biogeochemical effects. However, very few studies have investigated the  
70 effect of oxygen on hydrolytic rates, so far. Hoppe et al. (1990) did not find differences between oxic and anoxic  
71 incubations of Baltic Sea water. In the Cariaco Basin, hydrolytic rates were significantly higher in oxic compared to  
72 anoxic water (Taylor et al., 2009). However, this difference did not persist after rates were normalized to particulate  
73 organic matter concentration. The dependence of hydrolysis rates on organic matter concentrations described by Taylor  
74 et al. (2009), suggest that productivity may play a role for extracellular enzymatic rates in oxygen depleted systems.  
75 The Peruvian upwelling system displays high amounts of labile organic matter (Loginova et al., 2019) at shallow  
76 oxyclines and thus allows for studying effects of low oxygen on extracellular enzyme rates under substrate replete  
77 conditions. In general, combined investigations of extracellular enzyme rates, bacterial production (measured by  $^3\text{H}$   
78 leucine-incorporation) and carbon fluxes sampled at various *in situ* oxygen concentrations are still missing. These data,  
79 however, are crucial to inform ocean biogeochemical models that aim at quantification of  $\text{CO}_2$  uptake and nitrogen  
80 loss processes in oxygen depleted areas.

81 We studied bacterial degradation of organic matter in the OMZ off Peru during an extensive sampling campaign in the  
82 Austral winter 2017. We determined rates of total and cell-specific bacterial production ( $^3\text{H}$  leucine-incorporation) as  
83 well as of leucine aminopeptidase (LAPase) and  $\beta$ -glucosidase (GLUCase). We estimate bacterial utilisation of DOC  
84 supplied by diapycnal transport into the OMZ and discuss the contribution of bacterial degradation activity to the  
85 formation and persistence of the OMZ off Peru.

## 86 2. Methods

### 87 2.1. Study site and CTD measurements

88 Samples were taken during the cruises M136 and M138 on the R/V METEOR off Peru in April and June 2017,  
89 respectively (Fig. 1). Seawater was sampled with 24 Niskin bottles (10 L) on a general oceanic rosette system. At each  
90 station, 5 to 11 depths were sampled between 3 and 800 m (supplementary Table 1). Oxygen concentrations,  
91 temperature and depth were measured with a Sea-Bird SBE 9-plus CTD System (Sea-Bird Electronics, Inc., USA).  
92 Oxygen concentrations at each depth were determined with a SBE 43 oxygen sensor, calibrated with Winkler titrations  
93 (Winkler, 1888), resulting in an overall accuracy of  $1.5 \mu\text{mol kg}^{-1}$  oxygen. Chl  $a$  fluorescence was detected with a  
94 WETStar Chl  $a$  sensor (WET Labs, USA) and converted to  $\mu\text{g l}^{-1}$  using factors given by the manufacturer (Wetlabs).

95           **2.2. Dissolved organic carbon, total dissolved nitrogen, dissolved hydrolysable amino**  
96           **acids and dissolved high molecular weight carbohydrates**

97    DOC and total dissolved nitrogen (TDN) samples were taken at all stations, whereas the further analysis of DOC data  
98    was limited to stations with compatible bacterial production data and turbulence measurements (stations G-T). For  
99    DOC and TDN 20 ml of seawater was sampled in replicates, whereas both replicates were only analysed in case of  
100    conspicuous data. Samples were filtered through a syringe filter (0.45  $\mu\text{m}$  glass microfiber GD/X membrane, Whatman  
101    <sup>TM</sup>) that was rinsed with 50 ml sample, into a combusted glass ampoule (8 h, 500 °C). Before sealing the ampules, 20  
102     $\mu\text{l}$  of 30 % ultrapure hydrochloric acid were added. Samples were stored at 4 °C in the dark for 3 months until analyses.  
103    DOC and TDN were analysed using a TOC–VCSH with a TNM-1 detector (Shimadzu), applying a high-temperature  
104    catalytic oxidation method modified from Sugimura and Suzuki (1988). The instrument was calibrated with potassium  
105    hydrogen phthalate standard solutions (0 to 416.7  $\mu\text{mol C l}^{-1}$ ) (Merck 109017) and a potassium nitrate standard solution  
106    (0-57.1  $\mu\text{mol N l}^{-1}$ ) (Merck 105065). The instrument blank was examined with reference seawater standards (Hansell  
107    laboratory RSMAS University of Miami). The relative standard deviation (RSD) between repeated measurements is  
108    <1.1 % and <3.6 % and the detection limit is 1  $\mu\text{mol l}^{-1}$  and 2  $\mu\text{mol l}^{-1}$  for DOC and TDN, respectively.

109    At each station replicate 4 ml and 16 ml sample for the analysis of dissolved amino acids (DHAA) and dissolved  
110    combined carbohydrates (DCHO) were filtered through rinsed Acrodisc® 0.45 $\mu\text{m}$  GHP membrane (Pall) and stored  
111    in combusted vials (8 h, 500 °C) at -20 °C, respectively. Replicates were only analysed, if the first sample analyses  
112    resulted conspicuous data. The following DHAA were analysed: Alanine, Arginine, Glycine, Leucine, Phenylalanine,  
113    Serine, Threonine, Tyrosine, Valine, Aspartic acid + Asparagine (co-eluted), Glutamine + Glutamic acid (co-eluted),  
114     $\gamma$ -Aminobutyric acid and Isoleucine. DHAA samples were analysed with a high performance liquid chromatograph  
115    (1260 HPLC system, Aglient Technologies) using a C<sub>18</sub> column (Phenomex Kinetex) after in line ortho-  
116    phthaldialdehyde derivatization with mercaptoethanol after Lindroth and Mopper (1979) and Dittmar et al. (2009) with  
117    slight modifications after Engel and Galgani (2016). DCHO samples were desalted by membrane dialysis (1kDa,  
118    Spectra Por) and analysed with a high performance anion exchange chromatography (HPAEC) (DIONEX  
119    ICS3000DC) after Engel and Händel (2011). Detection limit of DHAA was 1.4 nmol L<sup>-1</sup> depending on amino acid and  
120    10 nmol L<sup>-1</sup> for DCHO. The precision was 2% and 5% for DHAA and DCHO, respectively.

121           **2.3. Diapycnal fluxes of oxygen and dissolved organic carbon**

122    In this study, we calculated DOC and oxygen loss rates (mmol m<sup>-3</sup> d<sup>-1</sup>) from the changes in diapycnal fluxes over depth.  
123    Therefore, oxygen and DOC profiles were used (stations G-T), excluding the mixed layer, defined by temperature  
124    deviating  $\leq 0.2^\circ\text{C}$  from the maximum, but excluding at least the upper 10 m. The diapycnal flux ( $\Phi_S$ ) was calculated  
125    for each CTD profile (Fischer et al., 2013; Schafstall et al., 2010) assuming a constant gradient between two sampled  
126    depths for DOC and oxygen:

127           1.  $\Phi_S = -K_p \nabla C_S$

128 where  $\nabla C_s$  is the gradient (mol m<sup>-4</sup>). The diapycnal diffusivity of mass ( $K \rho$ ) (m<sup>2</sup> s<sup>-1</sup>) was assumed to be constant  
129 (10<sup>-3</sup> m<sup>2</sup> s<sup>-1</sup>), which is reasonable compared with turbulence measurements by a freefalling microstructure probe  
130 (see supplementary methods and Fig. 2a). DOC loss rates ( $\nabla \Phi_{DOC}$ ; mmol m<sup>-3</sup> d<sup>-1</sup>) and oxygen loss rates ( $\nabla \Phi_{DO}$ ; mmol  
131 m<sup>-3</sup> d<sup>-1</sup>) were assumed to be equal to the negative vertical divergence of  $\Phi$ s calculated from the mean diapycnal flux  
132 profile, implying all other physical supply processes to be negligible.

#### 133 2.4. Bacterial abundance

134 Bacterial abundance was sampled in replicates at each station, whereas replicates were only analysed in exceptions.  
135 Abundance was determined by flow cytometry after Gasol and Del Giorgio (2000) from 1.6 ml sample, fixed with  
136 0.75 µl 25 % glutaraldehyde on board and stored at -80°C for maximal 3 month until analyses. Prior to analysis samples  
137 were thawed and 10 µL Flouresbrite® fluorescent beads (Polyscience, Inc.) and 10 µL Sybr Green (Invitrogen) (final  
138 concentration: 1x of the 1000x Sybr Green concentrate) were added to 400 µl sample. Cells were counted on a FACS  
139 Calibur (Becton Dickinson), calibrated with TruCount Beads™ (BD) with a measurement error of 2 % RSD.

#### 140 2.5. Bacterial production, oxygen demand and growth efficiency

141 For bacterial production, the incorporation of radioactive labelled leucine (<sup>3</sup>H) (specific activity 100 Ci mmol<sup>-1</sup>,  
142 Biotrend) was measured (Kirchman et al., 1985; Smith and Azam, 1992) at all depths of stations G-T as replicates. For  
143 this, the radiotracer at a saturating final concentration of 20 nmol l<sup>-1</sup> was added to 1.5 ml of sample and incubated for  
144 3 hours in the dark at 13°C. Controls were poisoned with trichloracetic acid. Samples were measured with a liquid  
145 scintillation counter (Hidex 300 SL, TriathalerTM, FCI). Samples taken at *in situ* oxygen concentrations of < 5 µmol  
146 kg<sup>-1</sup> were incubated under anoxic conditions by gentle bubbling with gas (0.13 % CO<sub>2</sub> in pure N<sub>2</sub>). Samples from oxic  
147 waters were incubated with head space, without bubbling. All samples were shacked thoroughly in between, therefore  
148 the bubbling of just one treatment won't have any effect. <sup>3</sup>H-leucine uptake was converted to carbon units applying a  
149 conversion factor of 1.5 kg C mol<sup>-1</sup> leucine (Simon and Azam, 1989). An analytical error of 5.2 % RSD was estimated  
150 with triplicate calibrations. Samples with a SD (standard deviation) > 30% between replicates were excluded.

151 The incubation of samples at a constant temperature of 13°C resulted in deviations of max. 11°C between incubation  
152 ( $T_{incubation}$ ) and *in situ* temperatures ( $T_{insitu}$ ). In order to estimate *in situ* bacterial production from measured bacterial  
153 production during incubations, measured temperature differences were taken into account following the approach of  
154 López-Urrutia and Morán (2007). First, the temperature difference between  $T_{insitu}$  and  $T_{incubation}$  ( $\delta T$ ) was computed in  
155 electron volt (eV<sup>-1</sup>), after  $T_{insitu}$  and  $T_{incubation}$  (K) had been multiplied with the Boltzmann's constant  $k$  (8.62x10<sup>-5</sup> eV K<sup>-1</sup>):

157 2.  $\delta T [eV^{-1}] = \frac{1}{T_{incubation}[K] \times k [eV K^{-1}]} - \frac{1}{T_{insitu}[K] \times k [eV K^{-1}]}$

158 The decadal logarithm of *in situ* bacterial production ( $\log_{10} BP_{insitu}$ ) was then calculated from the decadal logarithm of  
159 measured bacterial production during incubations ( $\log_{10} BP_{incubation}$ ). Therefore we applied three different factors ( $F$ )

160 depending on *in situ* Chl *a* concentration as proposed by López-Urrutia and Morán (2007); with *F* being -0.583, -0.5  
161 and -0.42 [ $fgCcell^{-1}d^{-1}ev$ ] for <0.5, 0.5-2 and >2  $\mu\text{g Chl } a \text{ L}^{-1}$ , respectively:

162

163 3.  $\log_{10}BP_{insitu}[fgCcell^{-1}d^{-1}] =$

164 
$$\log_{10}BP_{incubation}[fgCcell^{-1}d^{-1}] + \delta T [ev^{-1}]x F [fgCcell^{-1}d^{-1}ev]$$

165 Within the text, figures, equations and statistic results it is always referred to temperature corrected *in situ* bacterial  
166 production. Temperature corrected bacterial production and original bacterial production measured during incubation  
167 can be compared in supplementary Table 2.

168 The bacterial oxygen demand (BOD;  $\text{mmol O}_2 \text{ m}^{-3} \text{ d}^{-1}$ ) is the amount of oxygen needed to fully oxygenize organic  
169 carbon that has been taken up and not transformed into biomass by bacterial production ( $\text{mmol C m}^{-3} \text{ d}^{-1}$ ). The BOD  
170 was calculated as the difference between the estimated bacterial DOC uptake and the bacterial production applying a  
171 respiratory quotient (*cf*) of 1 (Eq. (4)) (Del Giorgio and Cole, 1998).

172 4.  $BOD = (DOC \text{ uptake} - \text{bacterial production}) \times cf$

173 The bacterial DOC uptake was calculated under two different assumptions: i) the DOC uptake by bacteria equals the  
174 DOC loss rate over depth or ii) the bacterial growth efficiency (BGE) follows the established temperature dependence  
175 ( $BGE=0.374[\pm 0.04] - 0.0104[\pm 0.002]T [\text{ }^{\circ}\text{C}]$ ), resulting in a BGE between 0.1 and 0.3 in the depth range of 10-60 m  
176 and an *in situ* temperature of 14 to 19 $^{\circ}\text{C}$  (Rivkin and Legendre, 2001) and can be used to estimate the bacterial DOC  
177 uptake from bacterial production (Eq. (5)).

178 5.  $bacterial \text{ DOC uptake} = \frac{bacterial \text{ production}}{BGE}$

179 **2.6.Extracellular enzyme rates**

180 Potential hydrolytic rates of LAPase and GLUCase were determined with fluorescent substrate analogues (Hoppe,  
181 1983). L-leucine-7-amido-4-methylcoumarin (Sigma Aldrich) and 4-methylumbelliferyl- $\beta$ -D-glucopyranoside (Acros  
182 Organics) were added in final concentrations of 1, 5, 10, 20, 50, 80, 100 and 200  $\mu\text{mol l}^{-1}$  in black 69 well plates  
183 (Costar) and kept frozen for at most one day until replicates of 200  $\mu\text{l}$  sample were added. After 0 and 12 hours of  
184 incubation at 13 $^{\circ}\text{C}$  in the dark, fluorescence was measured with a plate reader fluorometer (FLUOstar Optima, BMG  
185 labtech) (excitation: 355 nm; emission: 460 nm). An error of 2 % RSD was defined using the calibration with  
186 triplicates. Blanks with MilliQ were performed to exclude an increase in substrate decay over time.

187 Samples were collected in replicates ( $n=2$ ) at station A-K and incubated directly after sampling under oxygen  
188 conditions resembling *in situ* oxygen conditions. For samples > 5  $\mu\text{mol in situ O}_2 \text{ kg}^{-1}$  incubations were conducted  
189 under atmospheric oxygen conditions. Samples < 5  $\mu\text{mol in situ O}_2 \text{ kg}^{-1}$  were incubated in a gas tight incubator that  
190 had two openings to fill and flush it with gas. For our experiment the incubator was flushed and filled with N<sub>2</sub>, to  
191 reduce oxygen concentrations. Still control measurements occasionally revealed oxygen concentrations of 8 to 40  $\mu\text{mol}$

192  $\text{O}_2 \text{ kg}^{-1}$ . Additionally, samples were in contact with oxygen during pipetting and measurement. To investigate the  
193 influence of the different incubation methods we additionally incubated samples  $> 5 \mu\text{mol in situ O}_2 \text{ kg}^{-1}$  under reduced  
194 oxygen concentrations. On average incubations under reduced oxygen concentration yielded 2-27% higher values than  
195 those incubated under atmospheric oxygen conditions. However, the observed trends over depth remained similar (see  
196 supplementary discussion).

197 Calibration was conducted with 7-amino-4-methylcoumarin (2 nmol  $\text{l}^{-1}$  to 1  $\mu\text{mol l}^{-1}$ ) (Sigma Aldrich) and 4-  
198 methylumbellifereone (Sigma Aldrich) (16 nmol  $\text{l}^{-1}$  to 1  $\mu\text{mol l}^{-1}$ ) in seawater at atmospheric oxygen concentrations and  
199 under  $\text{N}_2$  atmosphere.

200 Maximum reaction velocity ( $V_{\max}$ ) at saturating substrate concentrations was calculated using both replicates at once,  
201 with the simple ligand binding function in SigmaPlot<sup>TM</sup> 12.0 (Systat Software Inc., San Jose, CA). Values for  $V_{\max}$   
202 with a SD  $> 30\%$  were excluded from further analyses. The degradation rate ( $\delta$ ) [ $\mu\text{mol C m}^{-3} \text{ d}^{-1}$ ] of DHAA by LAPase  
203 and DCHO by GLUCase was calculated after Piontek et al. (2014):

204 6. 
$$\delta = \frac{h_r * c}{100}$$

205 where  $h_r$  [%  $\text{d}^{-1}$ ] is the hydrolyses turnover at  $10^3 \mu\text{mol m}^{-3}$  substrate concentration and  $c$  is the carbon content of  
206 DHAA [ $\mu\text{mol C m}^{-3}$ ]. Measurements of  $h_r$  with a SD between duplicates of more than 30% were excluded. The same  
207 procedure was conducted with the carbon content of dissolved hydrolysable leucine, instead of DHAA, to account for  
208 variations in leucine concentrations, which is the main amino acid hydrolysed by LAPase.

209 Similar to bacterial production, *in situ* extracellular enzyme rates were estimated based on extracellular enzyme rates  
210 measured during incubation. To account for the differences between *in situ* and incubation temperatures a correction  
211 factor ( $F$ ) was applied based on differences in extracellular enzyme rates after additional incubations at  $22.4^\circ\text{C}$  next to  
212 the regular incubations at  $13^\circ\text{C}$  at five stations during the cruises. The fluorescence signals at different substrate  
213 concentrations increased on average by a factor of 0.05 and 0.03 ( $^\circ\text{C}^{-1}$ ) for GLUCase and LAPase, respectively. Under  
214 the assumption that the increase in rates with temperature was linear, measured enzyme rates were adapted to *in situ*  
215 temperature, with ( $EER_{\text{insitu}}$ ;  $\text{nmol L}^{-1} \text{ h}^{-1}$ ) and ( $EER_{\text{incubation}}$ ) being the *in situ* extracellular enzyme rates and  
216 extracellular enzyme rates during incubation, respectively:

217 7. 
$$\delta T [^\circ\text{C}] = T_{\text{insitu}} [^\circ\text{C}] - T_{\text{incubation}} [^\circ\text{C}]$$

218

219 8. 
$$EER_{\text{insitu}} [\text{nmol L}^{-1} \text{ h}^{-1}] =$$

220

221 
$$EER_{\text{incubation}} [\text{nmol L}^{-1} \text{ h}^{-1}] + EER_{\text{incubation}} [\text{nmol L}^{-1} \text{ h}^{-1}] \times F [^\circ\text{C}^{-1}] \times \delta T [^\circ\text{C}]$$

222 Within the text, figures, equations and statistic results it is always referred to the temperature corrected *in situ*  
223 extracellular enzyme rates. Temperature corrected extracellular enzyme rates and original extracellular enzyme rates  
224 measured during incubation can be compared in supplementary Table 2.

225 **2.7. Data analyses**

226 Data were plotted with Ocean Data View 4.74 (Schlitzer, 2016), MATLAB (8.3.0.532 (R2014a)) and R version 3.4.2  
227 using the package *ggplot2* (Hadley Wickham, 2016; R Development Core Team, 2008). Statistical significances  
228 between different regimes (see supplementary Table 2 for mean and SD within different regimes and statistical results)  
229 were tested with a *Wilcoxon test* (W) and correlation with the *Spearman Rank correlation* (S) in R version 3.4.2 (R  
230 Development Core Team, 2008) using following R packages: *FSA*, *car* and *multcomp* (Derek H. Olge, 2018; Horthorn  
231 et al., 2008; John Fox and Sanford Weisberg, 2011). For this extracellular enzyme data of station A-K and bacterial  
232 production data of station G-T were used, since not all parameters could be sampled at all depth. Diapycnal fluxes of  
233 DOC and oxygen were calculated with MATLAB (8.3.0.532 (R2014a)) and the Toolbox Gibbs SeaWater (GSW)  
234 Oceanographic Toolbox (3.05) (McDougall and Barker, 2011).

235 Samples were categorized into different oxygen regimes. Due to sensitivities of oxygen measurements, we did not  
236 distinguish between anoxic and suboxic regimes, but defined the suboxic “OMZ” oxygen regime by a threshold  $\leq 5$   
237  $\mu\text{mol O}_2 \text{ kg}^{-1}$  (Gruber, 2011). We defined the oxycline as one regime ( $>5$  to  $<60 \mu\text{mol O}_2 \text{ kg}^{-1}$ ) including the upper and  
238 lower oxycline or separated it into “low\_hypoxic” ( $>5$  to  $<20 \mu\text{mol O}_2 \text{ kg}^{-1}$ ) and “high\_hypoxic” ( $>20$  to  $<60 \mu\text{mol O}_2$   
239  $\text{kg}^{-1}$ ) regimes, representing important thresholds of oxygen concentrations for biological processes (Gruber, 2011).  
240 Oxygen concentrations  $>60 \mu\text{mol O}_2 \text{ kg}^{-1}$  were defined as “oxic”. Moreover, we partly differentiated between oxygen  
241 regimes situated above and below the OMZ (see supplementary Table 2 for results).

242 **3. Results**243 **3.1. Biogeochemistry of the Peruvian OMZ**

244 During our two cruises to the Peruvian upwelling system (Fig. 1), maximum Chl *a* concentration was higher and  
245 temperatures were warmer in April compared to June 2017, probably representing seasonal variability. Chl *a*  
246 concentration reached up to 11 and 4  $\mu\text{g l}^{-1}$  within the upper 25 m in April and June, respectively. Still, average Chl *a*  
247 concentration at depth  $<10$  m (M136:  $3.1 \pm 2.6 \mu\text{g l}^{-1}$ ; M138:  $2.8 \pm 1.3 \mu\text{g l}^{-1}$ ) were not significantly different between  
248 the two cruises. At depths  $>50$  m, Chl *a* concentration was generally below detection limit (Fig. 3a, supplementary  
249 Fig. 1). At depth  $< 10$  m the water was warmer in April ( $21.3 \pm 1.6^\circ\text{C}$ ) than in June ( $17.6 \pm 0.6^\circ\text{C}$ ) (Fig. 3b,  
250 supplementary Fig. 1). Oxygen concentration  $>100 \mu\text{mol kg}^{-1}$  was observed in the surface mixed layer. Oxygen  
251 decreased steeply with depth, reached suboxic concentrations ( $<5 \mu\text{mol kg}^{-1}$ ) at  $> 60 \pm 24$  m (Fig. 2c, 4a and 5a,  
252 supplementary Fig. 1) and fell below detection of Winkler titration. For further analysis and within the text *in situ*  
253 oxygen concentrations  $<5 \mu\text{mol O}_2 \text{ kg}^{-1}$  are referred to as “suboxic”. Shallowest depth with suboxic oxygen  
254 concentrations was 14 m in April (station Q) and 29 m in June (station D), probably representing that station Q was  
255 situated closer to the shore than station D. Oxygen increased again to up to  $15 \mu\text{mol kg}^{-1}$  at  $>500$  m (Fig. 4a and 5a,  
256 supplementary Fig. 1). TDN concentrations increased with depth from  $18 \pm 8 \mu\text{mol l}^{-1}$  and  $22 \pm 7 \mu\text{mol l}^{-1}$  within the  
257 upper 20 m in April and June, respectively, and reached a maximum of  $54 \mu\text{mol l}^{-1}$  at 850 m (Fig. 3c). DOC decreased  
258 with depth from  $94 \pm 37 \mu\text{mol l}^{-1}$  and  $69 \pm 12 \mu\text{mol l}^{-1}$  in the upper 20 m in April and June, respectively, to lowest values

259 of  $37 \mu\text{mol l}^{-1}$  at 850 m. The steepest gradient in DOC concentration was observed in the upper 20-60 m (Fig. 2b and  
260 3d) during both cruises.

261 **3.2. Bacterial production and enzymatic activity**

262 Bacterial production varied strongly throughout the study region and ranged from 0.2 to  $2404 \mu\text{mol C m}^{-3} \text{d}^{-1}$  (Fig. 4b),  
263 decreased in general from surface to depth (except for the most coastal station) and showed significantly higher rates  
264 in the oxygenated surface compared to the OMZ (Fig. 4b). At the most coastal station (G) bacterial production remained  
265 high near the bottom depth of 75 m ( $280 \mu\text{mol C m}^{-3} \text{d}^{-1}$  at 72 m) (Fig. 4b). Bacterial production did not differ  
266 significantly between the oxyclines and the suboxic core waters, neither off-shore (suboxic:  $0.3\text{-}127 \mu\text{mol C m}^{-3} \text{d}^{-1}$  ;  
267 oxyclines:  $1\text{-}304 \mu\text{mol C m}^{-3} \text{d}^{-1}$ ) nor at the most coastal stations (G and T) (suboxic:  $146\text{-}281 \mu\text{mol C m}^{-3} \text{d}^{-1}$  ) (oxycline:  
268  $74\text{-}452 \mu\text{mol C m}^{-3} \text{d}^{-1}$ ) (see supplementary Table 2 for all statistical results). Further, no significant correlation was  
269 observed between bacterial production and oxygen at *in situ*  $<20 \mu\text{mol O}_2 \text{ kg}^{-1}$ . Additionally, significantly lower  
270 bacterial production was observed within the lower oxycline ( $0.7\text{-}3.3 \mu\text{mol C m}^{-3} \text{d}^{-1}$ ) compared to the core OMZ ( $0.3\text{-}$   
271  $281 \mu\text{mol C m}^{-3} \text{d}^{-1}$ ) even though oxygen increased from  $<5$  to  $15 \mu\text{mol kg}^{-1}$  (Fig. 4a, b). Trends between oxygen  
272 regimes were similar between temperature corrected bacterial production (presented throughout the text) and original  
273 bacterial production measured during incubation (supplementary Table 2).

274 Overall, bacterial abundance ranged from 1 to  $49 \times 10^5 \text{ cells ml}^{-1}$ , with highest abundance observed at the surface and  
275 close to the sediment. Cell abundance in the oxyclines ( $1\text{-}16 \times 10^5 \text{ cells ml}^{-1}$ ) was significantly lower than in the OMZ  
276 core ( $1\text{-}25 \times 10^5 \text{ cells ml}^{-1}$ ) (Fig. 4c). A sharp decrease in bacterial abundance was observed below the OMZ.

277 Estimates for the *in situ* degradation rate of DHAA by LAPase take into account the available concentrations of DHAA  
278 and varied between 0.7 and  $39.7 \mu\text{mol C m}^{-3} \text{d}^{-1}$ . LAPase degradation rates observed within the OMZ core ( $5.5 \pm 2.1$   
279  $\mu\text{mol C m}^{-3} \text{d}^{-1}$ ) were significantly higher than in the oxyclines ( $3.1 \pm 2.3 \mu\text{mol C m}^{-3} \text{d}^{-1}$ ) (Fig. 5b). To exclude an  
280 influence of changing DHAA composition over depth, LAPase activity was also calculated using *in situ* concentrations  
281 of dissolved hydrolysable leucine instead of total DHAA. Degradation rates of dissolved hydrolysable leucine by  
282 LAPase ( $0.01\text{-}1.92 \mu\text{mol C m}^{-3} \text{d}^{-1}$ ) showed the same trend with significantly higher rates in suboxic waters than in the  
283 oxyclines. Thus, differences in the molecular composition of DHAA had no influence on spatial degradation patterns  
284 being higher in suboxic waters than in the upper oxycline. In contrast, degradation rates of DCHO ( $>1\text{kDa}$ ) were  
285 slightly reduced within the suboxic waters ( $0.69 \pm 1.30 \mu\text{mol C m}^{-3} \text{d}^{-1}$ ) compared to the oxyclines ( $1.1 \pm 1.0 \mu\text{mol C}$   
286  $\text{m}^{-3} \text{d}^{-1}$ ) (Fig. 5c). Since degradation rates were calculated by multiplying enzyme rates and carbon concentrations of  
287 DCHO and DHAA at *in situ* depth, differences in carbon concentrations are important for further interpretation. *In situ*  
288 carbon concentrations of DHAA were similar between the OMZ core ( $0.53 \pm 0.1 \mu\text{mol C L}^{-1}$ ) and the oxycline ( $0.57 \pm$   
289  $0.2 \mu\text{mol C L}^{-1}$ ). In contrast, *in situ* carbon concentrations of DCHO were reduced within the OMZ core ( $1.3 \pm 0.4$   
290  $\mu\text{mol C L}^{-1}$ ) compared to the oxycline ( $1.5 \pm 0.6 \mu\text{mol C L}^{-1}$ ) (Fig. 3e, f), suggesting that calculated differences between  
291 degradation rates may be influenced by different carbon concentrations. Potential hydrolytic rates at saturating  
292 substrate concentration ( $V_{\text{max}}$ ) of LAPase ranged between 9 and  $158 \text{ nmol l}^{-1} \text{ h}^{-1}$  and were  $\sim 30$  times lower for  
293 GLUCase. LAPase  $V_{\text{max}}$  was significantly higher within the suboxic waters ( $50 \pm 21 \text{ nmol l}^{-1} \text{ h}^{-1}$ ) compared to the  
294 oxycline ( $36 \pm 20 \text{ nmol l}^{-1} \text{ h}^{-1}$ ) and GLUCase  $V_{\text{max}}$  was more similar within the suboxic waters ( $1.6 \pm 1.5 \text{ nmol l}^{-1} \text{ h}^{-1}$ )

295 compared to the oxycline ( $1.2 \pm 0.6 \text{ nmol l}^{-1} \text{ h}^{-1}$ ) (Fig. 5d, e). Trends between oxygen regimes were similar between  
296 temperature corrected extracellular enzyme rates (presented throughout the text) and extracellular enzyme rates  
297 measured during incubation (supplementary Table 2).

298 To investigate physiological effects of suboxia, we normalized bacterial production and enzymatic rates to cell  
299 abundance. Cell-specific production ranged between 1 and 1120 amol C cell $^{-1}$  d $^{-1}$  (Fig. 4d). In contrast to total  
300 production, cell-specific production was significantly higher at the oxyclines compared to suboxic core waters at the  
301 off-shore stations (suboxic:  $1\text{-}102 \mu\text{mol C m}^{-3} \text{ d}^{-1}$ , oxyclines:  $6\text{-}219 \mu\text{mol C m}^{-3} \text{ d}^{-1}$ ). At the most coastal stations (G  
302 and T) cell-specific rates were more similar between suboxic waters and the oxyclines (suboxic:  $129\text{-}135 \mu\text{mol C m}^{-3}$   
303 d $^{-1}$ ) (oxycline:  $72\text{-}284 \mu\text{mol C m}^{-3} \text{ d}^{-1}$ ). Further, cell-specific bacterial production was slightly correlated (spearman  
304 rank correlation =0.36) to oxygen concentrations at  $\leq 20 \mu\text{mol O}_2 \text{ kg}^{-1}$  and as long as the most coastal stations (G and  
305 T) were included this correlation was significant (Fig. 4d, supplementary Table 2). A detailed view at total- and cell-  
306 specific bacterial production in dependence of *in-situ* oxygen concentrations, reveals a stronger increase of cell-specific  
307 bacterial production, especially at  $< 10 \mu\text{mol O}_2 \text{ kg}^{-1}$  at different stations (supplementary Fig. 2).

308 Cell-specific degradation rates of DHAA increased with depth and yielded significantly higher rates at the lower  
309 oxycline compared to all shallower depths. Cell-specific LAPase V<sub>max</sub>, GLUCase V<sub>max</sub> and GLUCase degradation rate  
310 showed the same trends, however for the latter this trend was not significant (Fig. 5g-j, supplementary Table 2)

### 311 **3.3. Bacterial contribution to the loss of dissolved organic carbon and oxygen in the oxycline**

312 We calculated the loss of oxygen and DOC during physical transport from below the mixed layer depth (MLD; 10-32  
313 m) to 60 m based on observed changes in diapycnal fluxes (Eq. (1), Fig. 2b, c). We estimated the bacterial contribution  
314 to this loss using two different approaches (Table 1): i) We assumed that the loss of DOC over depth equalled the  
315 bacterial uptake implying that the DOC is subsequently incorporated as bacterial biomass (bacterial production) or  
316 respired to CO<sub>2</sub> (Eq. (4)) ii) the amount of DOC taken up by bacteria was determined by the measured bacterial  
317 incorporation of carbon (bacterial production) and a constant ratio between carbon that is taken up and carbon that is  
318 incorporated as biomass (bacterial production) (Eq. (5)) (see section 2.5 for details). This ratio (BGE), was here  
319 assumed to be 10 or 30%, based on the empirical equation by Rivkin and Legendre with an *in situ* temperature that  
320 varied between 14 and 19°C (Rivkin and Legendre, 2001).

321 For total average DOC loss ( $\nabla\Phi_{DOC}$ ), we calculated a range of  $1.13\text{-}3.40 \text{ mmol C m}^{-3} \text{ d}^{-1}$ , with loss rates decreasing  
322 most strongly below the shallow mixed layer down to 40 m (Table 1, Fig. 2c). Following the first (i) assumption, all  
323 DOC that was lost over depth was taken up by bacteria and the measured bacterial production represents the fraction  
324 of DOC that was incorporated as biomass. Consequently, the remaining DOC that has been taken up, in other words  
325 the difference between DOC loss and bacterial production ( $0.03\text{-}0.71 \text{ mmol C m}^{-3} \text{ d}^{-1}$ ), was respired to CO<sub>2</sub> and  
326 represents the bacterial oxygen demand to account for the DOC loss (BOD<sub>E</sub>) ( $0.98\text{-}3.36 \text{ mmol O}_2 \text{ m}^{-3} \text{ d}^{-1}$ ) (Eq. (4)).  
327 Following this calculation, the BGE would vary between 1-21 % and 2 -13 % in the depth range of MLD-40 m and  
328 40-60 m, respectively, being on average almost constant over the two different depth ranges (6.6 and 5.0%). ii)  
329 Applying a BGE in the range of 10 and 30% and the measured bacterial production, the calculated bacterial DOC  
10

330 uptake $\phi$  was 0.08-7.10 mmol C m $^{-3}$  d $^{-1}$ . Hence, respiration of DOC to CO $_{2}$  accounted for a BOD $\phi$  of 0.06-6.39 mmol  
331 O $_{2}$  m $^{-3}$  d $^{-1}$  (Table 1).

332 **4. Discussion**

333 We investigated bacterial degradation of DOM by measuring bacterial production as an estimate for organic carbon  
334 transformation into biomass as well as rates of extracellular hydrolytic enzymes to provide information on the initial  
335 steps of organic matter degradation (Hoppe et al., 2002). We expected reduced rates of organic matter degradation  
336 within oxygen depleted waters, since reduced bacterial degradation activity might explain enhanced carbon fluxes in  
337 suboxic and anoxic waters (Devol and Hartnett, 2001). However, although bacterial production decreased with depth  
338 (Fig. 4b), this decrease was not related to oxygen concentrations. Moreover, no significant increase in bacterial  
339 production was observed at the lower oxycline, when oxygen concentration increased again (Fig. 4b). Decreasing  
340 bacterial production with depth has also been observed for fully oxygenated regions in the Atlantic (Baltar et al., 2009)  
341 and the equatorial Pacific (Kirchman et al., 1995) and has been explained by a decrease in the amount of bioavailable  
342 organic matter over depth.

343 The hypothesis of reduced bacterial degradation activity within the OMZ also implies reduced extracellular enzyme  
344 rates for the hydrolysis of organic matter. The extracellular enzymes rates of our study have to be interpreted carefully  
345 since incubation was not fully anoxic and the remaining oxygen might have biased the results. Still, we assume that  
346 most extracellular enzymes were present at the time of sampling and thus oxygen contamination during the incubations  
347 did not strongly influence the rate measurements. In our study, neither GLUCase nor LAPase V<sub>max</sub> were reduced within  
348 the suboxic waters compared to the oxyclines irrespective of incubation conditions (Fig. 5d, e, supplementary Fig. 3  
349 and 4). Thus, our findings show no evidence for reduced organic matter degradation in suboxic waters and are in good  
350 agreement with studies, which report similar bacterial degradation rates for oxic and suboxic waters (Cavan et al.,  
351 2017; Lee, 1992; Pantoja et al., 2009). Consequently, the hypothesis of enhanced carbon export in OMZ waters due to  
352 reduced organic matter degradation seems fragile and alternative explanations for enhanced carbon export efficiency  
353 e.g. reduced particle fragmentation due to zooplankton avoiding hypoxia (Cavan et al., 2017) may be more likely.  
354 Likewise, a reduced degradation of particulate organic carbon in suboxic waters as it is often assumed in global ocean  
355 biogeochemical models may have to be reconsidered (Ilyina et al., 2013).

356 Within OMZs dissolved nitrogen fuels e.g. denitrification or anaerobic ammonium oxidation (anammox) and is  
357 reduced to e.g. dinitrogen gas that evades to the atmosphere. Current estimates result in 20-50% of the total oceanic  
358 nitrogen loss occurring in OMZs (Lam and Kuypers, 2011). Meanwhile, a preferential degradation of amino acid  
359 containing organic matter in suboxic waters compared to oxic waters has been suggested (Van Mooy et al., 2002).  
360 Degradation of nitrogen compounds by heterotrophic bacteria (e.g. denitrifiers) in suboxic waters enables the release  
361 of ammonia and nitrite and subsequently may support anammox, an autotrophic anaerobic pathway (Babbin et al.,  
362 2014; Kalvelage et al., 2013; Lam and Kuypers, 2011; Ward, 2013). This interaction between denitrifiers and anammox  
363 bacteria could fuel the loss of nitrogen to the atmosphere. Our data indeed showed enhanced degradation of amino-  
364 acid-containing organic matter in low oxygen waters. Indicators for protein decomposition, i.e. LAPase V<sub>max</sub> and the

365 degradation rate of DHAA by LAPase, were more pronounced within the suboxic waters (Fig. 5b, d). Therefore,  
366 observed LAPase rates are in line with the hypothesis of preferential degradation of nitrogen compounds under suboxia.  
367 However, simultaneous rate measurements of protein hydrolysis, nitrate reduction (e.g. denitrification) and anammox  
368 are needed to prove an indirect stimulation of anammox by protein hydrolysis via denitrification. A close coupling  
369 between anammox and nitrate reducing bacteria has previously been shown for wastewater treatments. There, nitrate  
370 reducers directly take up organic matter excreted by the anammox bacteria which in turn benefit from the released  
371 nitrite by respiratory nitrate reduction (Lawson et al., 2017). In the Pacific, denitrifiers and anammox bacteria are  
372 separated in space and time (Dalsgaard et al., 2012), potentially weakening a direct inter-dependency.

373 To investigate physiological effects of suboxia, we normalized bacterial production and enzymatic rates to cell  
374 abundance and found higher cell-specific bacterial production near the oxycline compared to suboxic waters and  
375 highest cell-specific enzyme rates at the lower oxycline (Fig. 4d, 5g-j). Higher cell-specific bacterial production at  
376 oxic-anoxic interfaces in the water column has previously been reported for the Baltic Sea (Brettar et al., 2012). Baltar  
377 et al. (2009) showed increasing cell-specific enzymatic rates and decreasing cell-specific bacterial production, with  
378 increasing depth in the subtropical Atlantic and related this pattern to decreasing organic matter lability. In our study,  
379 differences in cell-specific bacterial production between suboxic waters and the oxycline did not persist at the most  
380 coastal stations (G and T). This indicates the stimulation of bacterial activity, including anaerobic respiratory processes,  
381 by the high input of labile organic matter. Therefore, our study suggests that a possible impairment of cell-specific  
382 bacterial production under suboxia is reduced by supply of organic matter. However, this hypothesis is restricted to a  
383 very limited number of samples and should be tested in further studies. While labile organic matter is decreasing with  
384 depth (e.g. Loginova et al., 2019), TDN (Fig. 3c), especially inorganic nitrogen is increasing with depth. Thus, high  
385 concentrations of inorganic nitrogen at the lower oxycline are available for heterotrophic and chemoautotrophic energy  
386 gains. For instance, the co-occurrence of nitrate reduction, that was still detected at  $25 \mu\text{mol O}_2 \text{ L}^{-1}$ , and microaerobic  
387 respiration might have stimulated cell-specific production or the accumulation of especially active bacterial species  
388 (Kalvelage et al., 2011, 2015).

389 Depth distribution of cell-specific and total bacterial production was different (Fig. 4b, d and supplementary Fig. 2);  
390 cell-specific production was significantly reduced in suboxic waters, while total production was more similar in  
391 suboxic waters compared to the oxycline. This suggests that lower cell-specific production was compensated by higher  
392 cell abundance within the suboxic waters (Fig. 4c), resulting in an overall unhampered bacterial organic matter cycling  
393 in the OMZ core. One reason for the accumulation of cells within the OMZ might be reduced predation, suggesting  
394 the OMZ core as an ecological niche for slowly growing bacteria. Reduced grazing by bacterivores thus preserves  
395 bacterial biomass in suboxic waters from entering into the food chain. This way of bacterial biomass preservation has  
396 been suggested as possible explanation for enhanced carbon preservation in anoxic sediments by Lee (1992), and may  
397 also explain our observations for the anoxic water column.

398 In general, bacterial community composition in OMZs has been shown to be strongly impacted by oxygen. In the OMZ  
399 near the shelf off Chile Arctic96BD-19 and SUP05 dominate heterotrophic and autotrophic groups in hypoxic waters  
400 (Aldunate et al., 2018). Next to the appearance of autotrophic bacteria that are related to sulphur (e.g. SUP05) or

401 nitrogen cycling (e.g. Planctomycetes), also bacteria related to cycling of complex carbohydrates have been discovered  
402 in OMZs (Callbeck et al., 2018; Galán et al., 2009; Thrash et al., 2017), and may explain the unaltered high potential  
403 ( $V_{max}$ ) of the extracellular enzymes GLUCase and heterotrophic bacterial production in suboxic waters in our study  
404 (Fig. 5e, 4b). For instance, SAR406, SAR202, ACD39 and PAUC34f have the genetic potential for the turnover of  
405 complex carbohydrates and anaerobic respiratory processes, in the Gulf of Mexico (Thrash et al., 2017). Consequently,  
406 our findings of active bacterial degradation of DOM are supported by molecular biological studies. Still, simultaneous  
407 measurements of bacterial degradation and production have to be combined with molecular analysis, in future studies  
408 off Peru.

409 Heterotrophic bacteria are the main users of marine DOM (Azam et al., 1983; Carlson and Hansell, 2015) and  
410 responsible for ~79% of total respiration in the Pacific Ocean (Del Giorgio et al., 2011), proposing that heterotrophic  
411 bacteria drive organic matter and oxygen cycling in the ocean and significantly contribute to the formation of the OMZ.  
412 Under the assumption that the calculated loss of DOC during diapycnal transport (<60 m) is caused solely by bacterial  
413 uptake and subtracting the amount of carbon channelled into biomass production, our study verifies the importance of  
414 bacterial DOC degradation for the formation of the OMZ. We estimated a BOD (0.98-3.36 mmol O<sub>2</sub> m<sup>-3</sup> d<sup>-1</sup>) that is in  
415 line with earlier respiration measurements in the upper oxycline off Peru (Kalvelage et al., 2015) and represents 18-  
416 33% of the oxygen loss over depth, implying a rather low average BGE (6.5 and 5.0 %) (Table 1). Calculating the  
417 bacterial uptake of DOC from production rates and a more conservative BGE between 10 and 30% as previously  
418 suggested (Rivkin and Legendre, 2001) for the *in situ* temperature of 14 to 19 °C, 3-209% of the DOC loss and 1-62%  
419 of oxygen loss could be attributed to bacterial degradation of DOM. The first approach reveals an average BGE (6.5  
420 and 5.0%) that is still within the range of previous reports for upwelling systems of the Atlantic (<1-58%) and  
421 northeastern Pacific (<10%) (Alonso-Sáez et al., 2007; Del Giorgio et al., 2011). The high variability in BGE is a topic  
422 of ongoing research. Until now 54% of the variability could be explained by variations in temperature (Rivkin and  
423 Legendre, 2001). Our data suggest that oxygen availability may be another control of BGE leading to rather low BGE  
424 in low oxygen waters. This is especially indicated by a low but rather constant average BGE (6.5 and 5.0%), which we  
425 estimated for the water column down to 60m depth under the assumption that all DOC that is lost over depth can be  
426 attributed to bacterial uptake. A low BGE might be explained by a bacterial community that has higher energetic  
427 demands, but in return is adapted to variable oxygen conditions. Additionally, the BGE is decreasing with an increasing  
428 carbon to nitrogen ratio of the available substrate (Goldman et al., 1987). In the OMZ off Peru the ratio between DOC  
429 and dissolved organic nitrogen is frequently high (~12 to 16) (Loginova et al., 2019), and might further contribute to  
430 the low BGE. High respiration rates induced by bacterial DOC degradation contribute to sustaining the OMZ, besides  
431 oxygen consumption by bacteria that hydrolyze and degrade particulate organic matter (Cavan et al., 2017). Another,  
432 but likely minor contribution to overall respiration is made by zooplankton and higher trophic levels (e.g. Kiko et al.,  
433 2016). Additionally, physical processes such as an intrusion of oxygen depleted waters by eddies, upwelling or  
434 advection, may add to the oxygen and DOC loss over depth (Brandt et al., 2015; Llanillo et al., 2018; Steinfeldt et al.,  
435 2015).

436 Uncertainties of our assumption that the loss of DOC is caused solely by bacterial uptake include other processes  
437 potentially contributing to DOC removal, but not taken into consideration here like DOC adsorption onto particles,

438 DOC uptake by eukaryotic cells or the physical coagulation of DOC into particles, e.g. by formation of gel-like  
439 particles such as transparent exopolymer particles and Coomassie stainable particles (Carlson and Hansell, 2015; Engel  
440 et al., 2004, 2005). Moreover, temporal variations in diapycnal fluxes may be large, as indicated by the confidence  
441 interval of solute fluxes (Fig. 2b, c) during this study and by 2 to 10 times lower DOC and oxygen loss rates during  
442 other seasons (Loginova et al., 2019). However, our study is the first combining physical and microbial rate  
443 measurements and gives estimates for carbon and oxygen losses in the upwelling system off Peru and can help  
444 improving current biogeochemical models by constraining bacterial DOM degradation.

445 Loginova et al. (2019) conducted similar physical rate measurements in the same study area with ~2 and ~10 times  
446 lower DOC and oxygen loss in the upper ~40 m compared to our study. Differences in loss rates were mainly caused  
447 by a ~ 10 times higher diapycnal diffusivity of mass in our study. This may have been caused by weaker stratification  
448 in the upper 100 m depth or differences in the turbulence conditions. Loginova et al. (2019) estimated a contribution  
449 of bacterial DOM degradation to oxygen loss (38 %) based on the loss of labile DOC (DHAA and DCHO). This value  
450 agrees well with our estimates of 18–33% of total oxygen loss, calculated under the assumption that DOC loss is solely  
451 attributed to bacterial degradation. However, the comparison of DOC and oxygen loss within each study revealed  
452 different patterns. Loginova et al. (2019) found a loss of DOC that clearly exceeded the loss of oxygen within the upper  
453 ~40 m. Hence, respiration of DOC could fully explain the observed oxygen loss in that study. In our study, more  
454 oxygen than DOC was lost over depth (Table 1). This loss of oxygen needs additional explanations such as degradation  
455 of particulate organic matter and physical mixing processes. One reason for the observed differences between the two  
456 studies that have been conducted in the same region might be seasonality. The study by Loginova et al. (2019) took  
457 place in austral summer, whereas our data were gained during austral winter. Water temperature was quite similar  
458 during both studies, probably due to the coastal El Niño one month before our sampling campaign (Garreaud, 2018).  
459 Still, the study by Loginova et al. (2019) included more stations with high Chl *a* concentrations (~8 µg L<sup>-1</sup>), as typical  
460 for the austral summer, indicating a more productive system with more labile DOM (DCHO and DHAA). Prevalence  
461 of more labile DOM might explain the higher contribution of microbial DOM respiration to oxygen loss in the study  
462 by Loginova et al. (2019). Additionally, Loginova et al. (2019) sampled with a much higher vertical resolution within  
463 the upper 140 m, restricting the direct comparability with our study.

464  
465 In oxygen depleted waters of the Peruvian upwelling system, the chemoautotrophic process of anammox has been  
466 assumed to dominate anaerobic nitrogen cycling (Kalvelage et al., 2013), with lower but more constant rates compared  
467 to more sporadically occurring heterotrophic denitrification (Dalsgaard et al., 2012). Our study points towards a  
468 widespread occurrence of heterotrophic denitrification processes in the Peruvian OMZ, since the here applied method  
469 for measuring bacterial production is restricted to heterotrophs. Our rates for bacterial production within the suboxic  
470 waters averaged to 37 µmol C m<sup>-3</sup> d<sup>-1</sup> (0.3–281 µmol C m<sup>-3</sup> d<sup>-1</sup>).

471  
472 We compared bacterial production, i.e. rates of carbon incorporation, with denitrification rates previously reported for  
473 the South Pacific. Therefore, we converted one mol of reduced nitrogen that were measured by Dalsgaard et al. (2012)  
474 and Kalvelage et al. (2013) to 1.25 mol of oxidized carbon after the reaction equation given by Lam and Kuypers

475 (2011). This calculation indicates that on average  $\leq 19 \mu\text{mol C m}^{-3} \text{ d}^{-1}$  are oxidized by denitrifying bacteria in the  
476 Eastern Tropical Pacific (Dalsgaard et al., 2012; Kalvelage et al., 2013).  
477 The amount of carbon oxidized by denitrification based on the studies of Dalsgaard et al. (2012) and Kalvelage et al.  
478 (2013) can be converted into bacterial production applying a BGE. The average temperature dependent BGE was 20%.  
479 A BGE of 20% agrees well with other studies (Del Giorgio and Cole, 1998). Assuming a BGE of 20%, the  
480 denitrification rates of Dalsgaard et al. (2012) and Kalvelage et al. (2013) suggest a bacterial production of  $\leq 5 \mu\text{mol}$   
481  $\text{C m}^{-3} \text{ d}^{-1}$ , equivalent to only about 14% of total average heterotrophic bacterial production in suboxic waters  
482 determined in our study. For the sum of anaerobic carbon oxidation rates including denitrification, DNRA and simple  
483 nitrate reduction,  $109 \mu\text{mol C m}^{-3} \text{ d}^{-1}$  ( $6-515 \mu\text{mol C m}^{-3} \text{ d}^{-1}$ ) may be expected for the Peruvian shelf, with the reduction  
484 of nitrate to nitrite representing the largest proportion ( $2-505 \mu\text{mol C}^{-1} \text{ m}^{-3} \text{ d}^{-1}$ ), based on the relative abundance of the  
485 different N-functional genes (Kalvelage et al., 2013). These anaerobic respiration measurements are equivalent to a  
486 bacterial production of  $\sim 27 \mu\text{mol C m}^{-3} \text{ d}^{-1}$  ( $1-129 \mu\text{mol C m}^{-3} \text{ d}^{-1}$ ) and are thus lower than our direct measurements of  
487 bacterial production rates. Moreover, the reduction of nitrate, could not be detected at every depth and incubation  
488 experiments partly showed huge variations over depth (Kalvelage et al., 2013), whereas we were able to measure  
489 bacterial production in every sample. The same calculation can be repeated assuming a BGE of 6%, which is the  
490 average BGE within this study based on DOC loss and bacterial production. Assuming a BGE of 6%, the estimated  
491  $109 \mu\text{mol C m}^{-3} \text{ d}^{-1}$  that are respired by anaerobic carbon oxidation (Kalvelage et al., 2013) would represent 94% of  
492 the carbon uptake. Consequently,  $7 \mu\text{mol C m}^{-3} \text{ d}^{-1}$ , i.e. 6% of the carbon uptake, are incorporated into the bacterial  
493 biomass. A bacterial biomass production of  $7 \mu\text{mol C m}^{-3} \text{ d}^{-1}$  is even lower than the bacterial production of  $27 \mu\text{mol C}$   
494  $\text{m}^{-3} \text{ d}^{-1}$ , based on a BGE of 20% and cannot explain the average bacterial production measured in suboxic waters during  
495 our study ( $37 \mu\text{mol C m}^{-3} \text{ d}^{-1}$ ). Therefore, this estimation suggests higher rates of heterotrophic anaerobic respiratory  
496 processes than previously measured. Since denitrification rates were not measured directly, the comparability of  
497 published denitrification rates and our measurements of bacterial production are limited. However, our data suggest  
498 that the carbon oxidation potential off Peru is more evenly horizontally and vertically distributed than expected and  
499 also corroborate earlier suggestions of unexpectedly high rates of heterotrophic nitrogen cycling in the OMZ off Peru  
500 based on observations of high concentrations of atmospheric nitrous oxide (Bourbonnais et al., 2017).

## 501 5. Conclusion

502 Our study suggests that suboxia does not reduce bacterial degradation of organic matter in the Eastern Tropical South  
503 Pacific off Peru. Bacterial species are seemingly adapted to these environments and higher cell abundance compensates  
504 for hampered cell-specific bacterial production under suboxia. Therefore, the previously observed enhanced carbon  
505 export in OMZs compared to oxygenated waters requires alternative explanations. Differences between cell-specific  
506 and total rates of bacterial activity allude to different controls of cell abundance in suboxic systems, highlighting the  
507 OMZ as a specific ecological niche. The combination of bacterial and physical rate measurements suggests that low  
508 BGEs in the upper oxycline contribute to sustaining the OMZ. Meanwhile, new findings during our study call for  
509 additional studies: i) DOC loss differed strongly between our investigation and the study of Loginova et al. (2019).  
510 Therefore, combined physical and biological rate measurements in the Peruvian upwelling system should be repeated  
511 during austral summer, to learn more about the interplay of DOC loss and bacterial production during different seasons.  
15

512 ii) Integrated measurements of denitrification, microaerobic respiration and bacterial production are needed to estimate  
513 the fractions of incorporated and respired carbon under suboxia. The BGE received in that way could support or  
514 disprove the low BGE estimate, which was calculated from DOC loss and bacterial production in our study.  
515 Consequently, our study highlights the need for a better mechanistic understanding and quantification of processes  
516 responsible for oxygen and DOM loss in OMZs that is inevitable to predict future patterns of deoxygenation in a  
517 warming climate.

518 *Data Availability.* PANGEA: 10.1594/PANGAEA.891247

519

520 *Author contributions.* M.M. and A.E. designed the scientific study, analysed the data and wrote the manuscript. J.L.  
521 calculated DOC and oxygen fluxes, G.K. sampled and calibrated the CTD data and both J.L. and G.K. commented on  
522 the manuscript.

523 *Competing interests.* The authors declare that they have no conflict of interest.

524 *Acknowledgments:* We thank Jon Roa, Tania Klüver and Ruth Flerus for the sampling and/or analysis of DOC/TDN;  
525 cell abundance, bacterial production and DHAA. Moreover, we would like to thank Judith Piontek, Sören Thomsen,  
526 Carolina Cisternas-Novoa and Frédéric A.C. Le Moigne who helped and gave advice for sampling during the cruises.  
527 We are grateful to the working group of Hermann Bange and Stefan Sommer who provided Winkler measurements.  
528 We thank the cruise leaders Hermann Bange and Marcus Dengler, crew, officers and the captains of the F.S. Meteor  
529 for the support on board and the successful cruises. This study was supported by the Helmholtz Association and by the  
530 Collaborative Research Center 754 / SFB Sonderforschungsbereich 754 ‘Climate-Biogeochemistry Interactions in the  
531 Tropical Ocean’.

532 **References**

533 Aldunate, M., De la Iglesia, R., Bertagnolli, A. D. and Ulloa, O.: Oxygen modulates bacterial community  
534 composition in the coastal upwelling waters off central Chile, *Deep. Res. Part II*, in press, 1–12,  
535 doi:10.1016/j.dsr2.2018.02.001, 2018.

536 Alonso-Sáez, L., Gasol, J. M., Arístegui, J., Vilas, J. C., Vaqué, D., Duarte, C. M. and Agustí, S.: Large-scale  
537 variability in surface bacterial carbon demand and growth efficiency in the subtropical northeast Atlantic Ocean,  
538 *Limnol. Oceanogr.*, 52(2), 533–546, doi:10.4319/lo.2007.52.2.0533, 2007.

539 Azam, F., Fenchel, T., Field, J. G., Gray, J. S., Meyer-Reil, L. A. and Thingstad, F.: The ecological role of water-  
540 column microbes in the sea., *Mar. Ecol. Prog. Ser.*, 10(3), 257–263, 1983.

541 Babbin, A. R., Keil, R. G., Devol, A. H. and Ward, B. B.: Organic matter stoichiometry, flux, and oxygen control  
542 nitrogen loss in the ocean, *Science.*, 344(406), 406–408, doi:10.1126/science.1248364, 2014.

543 Bakund, A. and Nelson, C. S.: The seasonal cycle of wind-stress curl in subtropical eastern boundary current  
544 regions., *J. Phys. Oceanogr.*, 21, 1815–1834, 1991.

545 Baltar, F., Arístegui, J., Sintes, E., van Aken, H. M., Gasol, J. M. and Herndl, G. J.: Prokaryotic extracellular  
546 enzymatic activity in relation to biomass production and respiration in the meso- and bathypelagic waters of the  
547 (sub)tropical Atlantic, *Environ. Microbiol.*, 11(8), 1998–2014, doi:10.1111/j.1462-2920.2009.01922.x, 2009.

548 Benner, R. and Amon, R. M. W.: The size-reactivity continuum of major bioelements in the ocean, *Ann. Rev. Mar.*  
549 *Sci.*, 7(1), 185–205, doi:10.1146/annurev-marine-010213-135126, 2015.

550 Boetius, A. and Lochte, K.: Effect of organic enrichments on hydrolytic potentials and growth of bacteria in deep-sea  
551 sediments., *Mar. Ecol. Prog. Ser.*, 140, 239–250, doi:10.3354/meps140239, 1996.

552 Bourbonnais, A., Letscher, R. T., Bange, H. W., Échevin, V., Larkum, J., Mohn, J., Yoshida, N. and Altabet, M. A.:  
553 N<sub>2</sub>O production and consumption from stable isotopic and concentration data in the Peruvian coastal upwelling  
554 system, *Global Biogeochem. Cycles*, 31(4), 678–698, doi:10.1002/2016GB005567, 2017.

555 Brandt, P., Bange, H. W., Banyte, D., Dengler, M., Didwischus, S., Fischer, T., Greatbatch, R. J., Hahn, J., Kanzow,  
556 T., Karstensen, J., Körtzinger, A., Krahmann, G., Schmidtko, S., Stramma, L., Tanhua, T. and Visbeck, M.: On the  
557 role of circulation and mixing in the ventilation of oxygen minimum zones with a focus on the eastern tropical North  
558 Atlantic, *Biogeoscience*, 12, 489–512, doi:10.5194/bg-12-489-2015, 2015.

559 Brettar, I., Christen, R. and Höfle, M. G.: Analysis of bacterial core communities in the central Baltic by comparative  
560 RNA–DNA-based fingerprinting provides links to structure–function relationships., *ISME J.*, 6(1), 195–212,  
561 doi:10.1038/ismej.2011.80, 2012.

562 Callbeck, C. M., Lavik, G., Ferdelman, T. G., Fuchs, B., Gruber-Vodicka, H. R., Hach, P. F., Littmann, S.,

563 Schoffelen, N. J., Kalvelage, T., Thomsen, S., Schunck, H., Löscher, C. R., Schmitz, R. A. and Kuypers, M. M. M.:  
564 Oxygen minimum zone cryptic sulfur cycling sustained by offshore transport of key sulfur oxidizing bacteria, *Nat.*  
565 *Commun.*, 9(1729), 1–11, doi:10.1038/s41467-018-04041-x, 2018.

566 Carlson, C. A. and Hansell, D. A.: DOM sources, sinks, reactivity, and budgets, in *Biogeochemistry of marine*  
567 *dissolved organic matter*, edited by C. A. Carlson and D. A. Hansell, pp. 65–126, Elsevier, London., 2015.

568 Cavan, E. L., Trimmer, M., Shelley, F. and Sanders, R.: Remineralization of particulate organic carbon in an ocean  
569 oxygen minimum zone, *Nat. Commun.*, 8, doi:10.1038/ncomms14847, 2017.

570 Cole, J. J. and Pace, M. L.: Bacterial secondary production in oxic and anoxic freshwaters, *Limnol. Oceanogr.*, 40(6),  
571 1019–1027, doi:10.4319/lo.1995.40.6.1019, 1995.

572 Czeschel, R., Stramma, L., Schwarzkopf, F. U., Giese, B. S., Funk, A. and Karstensen, J.: Middepth circulation of  
573 the eastern tropical South Pacific and its link to the oxygen minimum zone, *J. Geophys. Res.*, 116(C01015), 1–13,  
574 doi:10.1029/2010JC006565, 2011.

575 Dalsgaard, T., Thamdrup, B., Farías, L. and Revsbech, N. P.: Anammox and denitrification in the oxygen minimum  
576 zone of the eastern South Pacific, *Limnol. Oceanogr.*, 57(5), 1331–1346, doi:10.4319/lo.2012.57.5.1331, 2012.

577 Derek H. Olge: FSA: Fisheries Stock Analysis, 2018.

578 Devol, A. H. and Hartnett, H. E.: Role of the oxygen-deficient zone in transfer of organic carbon to the deep ocean,  
579 *Limnol. Oceanogr.*, 46(7), 1684–1690, doi:10.4319/lo.2001.46.7.1684, 2001.

580 Dittmar, T., Cherrier, J. and Ludichowski, K. U.: The analysis of amino acids in seawater., in *Practical guidelines for*  
581 *the analysis of seawater.*, edited by O. Wurl, pp. 67–78, CRC Press, Boca Raton., 2009.

582 Echevin, V., Aumont, O., Ledesma, J. and Flores, G.: The seasonal cycle of surface chlorophyll in the Peruvian  
583 upwelling system : A modelling study, *Prog. Oceanogr.*, 79(2–4), 167–176, doi:10.1016/j.pocean.2008.10.026, 2008.

584 Engel, A. and Galgani, L.: The organic sea-surface microlayer in the upwelling region off the coast of Peru and  
585 potential implications for air–sea exchange processes, *Biogeosciences*, 13(4), 989–1007, doi:10.5194/bg-13-989-  
586 2016, 2016.

587 Engel, A. and Händel, N.: A novel protocol for determining the concentration and composition of sugars in  
588 particulate and in high molecular weight dissolved organic matter (HMW-DOM) in seawater., *Mar. Chem.*, 127(1),  
589 180–191, doi:10.1016/j.marchem.2011.09.004, 2011.

590 Engel, A., Thoms, S., Riebesell, U., Rochelle-Newall, E. and Zondervan, I.: Polysaccharide aggregation as a  
591 potential sink of marine dissolved organic carbon, *Nature*, 428(6986), 929–932, doi:10.1038/nature02453, 2004.

592 Engel, A., Zondervan, I., Aerts, K., Beaufort, L., Benthien, A., Chou, L., Delille, B., Gattuso, J.-P., Harlay, J.,

593 Heemann, C., Hoffmann, L., Jacquet, S., Nejstgaard, J., Pizay, M.-D., Rochelle-Newall, E., Schneider, U.,  
594 Terbrueggen, A. and Riebesell, U.: Testing the direct effect of CO<sub>2</sub> concentration on a bloom of the coccolithophorid  
595 *Emiliania huxleyi* in mesocosm experiments, *Limnol. Oceanogr.*, 50(2), 493–507, doi:10.4319/lo.2005.50.2.0493,  
596 2005.

597 Fischer, T., Banyte, D., Brandt, P., Dengler, M., Krahmann, G., Tanhua, T. and Visbeck, M.: Diapycnal oxygen  
598 supply to the tropical North Atlantic oxygen minimum zone, *Biogeosciences*, 10(7), 5079–5093, doi:10.5194/bg-10-  
599 5079-2013, 2013.

600 Galán, A., Molina, V., Thamdrup, B., Woebken, D., Lavik, G., Kuyper, M. M. M. and Ulloa, O.: Anammox bacteria  
601 and the anaerobic oxidation of ammonium in the oxygen minimum zone off northern Chile, *Deep. Res. II*, 56, 1021–  
602 1031, doi:10.1016/j.dsr2.2008.09.016, 2009.

603 Garreaud, R. D.: A plausible atmospheric trigger for the 2017 coastal El Niño, *Int. J. Climatol.*, 38, 1296–1302,  
604 doi:10.1002/joc.5426, 2018.

605 Gasol, J. M. and Del Giorgio, P. A.: Using flow cytometry for counting natural planktonic bacteria and  
606 understanding the structure of planktonic bacterial communities, *Sci. Mar.*, 64(2), 197–224,  
607 doi:10.3989/scimar.2000.64n2197, 2000.

608 Del Giorgio, P. A. and Cole, J. J.: Bacterial growth efficiency in natural aquatic systems, *Annu. Rev. Ecol. Syst.*,  
609 29(May), 503–541, 1998.

610 Del Giorgio, P. A., Condon, R., Bouvier, T., Longnecker, K., Bouvier, C., Sherr, E. and Gasol, J. M.: Coherent  
611 patterns in bacterial growth, growth efficiency, and leucine metabolism along a northeastern Pacific inshore-offshore  
612 transect, *Limnol. Oceanogr.*, 56(1), 1–16, doi:10.4319/lo.2011.56.1.0001, 2011.

613 Goldman, J. C., Caron, D. A. and Dennett, M. R.: Regulation of gross growth efficiency and ammonium regeneration  
614 in bacteria by substrate C : N ratio., *Limnol. Oceanogr.*, 32(6), 1239–1252, doi:10.4319/lo.1987.32.6.1239, 1987.

615 Graco, M. I., Purca, S., Dewitte, B., Castro, C. G., Morón, O., Ledesma, J., Flores, G. and Gutiérrez, D.: The OMZ  
616 and nutrient features as a signature of interannual and low-frequency variability in the Peruvian upwelling system,  
617 *Biogeosciences*, 14(20), 4601–4617, doi:10.5194/bg-14-4601-2017, 2017.

618 Grossart, H., Allgaier, M., Passow, U. and Riebesell, U.: Testing the effect of CO<sub>2</sub> concentration on the dynamics of  
619 marine heterotrophic bacterioplankton, *Limnol. Oceanogr.*, 51(1), 1–11, doi:10.4319/lo.2006.51.1.0001, 2006.

620 Gruber, N.: Warming up, turning sour, losing breath : ocean biogeochemistry under global change., *Phil. Trans. R.  
621 Soc.*, 369(1943), 1980–1996, doi:10.1098/rsta.2011.0003, 2011.

622 Hadley Wickham: *ggplot2: Elegant Graphics for Data Analysis*, Springer-Verlag, New York., 2016.

623 Hoppe, H.-G.: Significance of exoenzymatic activities in the ecology of brackish water: measurements by means of

624 methylumbelliferyl-substrates., *Mar. Ecol. Prog. Ser.*, 11, 299–308, 1983.

625 Hoppe, H.-G., Gocke, K. and Kuparinen, J.: Effect of H<sub>2</sub>S on heterotrophic substrate uptake, extracellular enzyme  
626 activity and growth of brackish water bacteria., *Mar. Ecol. Prog. Ser.*, 64, 157–167, doi:10.3354/meps064157, 1990.

627 Hoppe, H.-G., Arnosti, C. and Herndl, G. F.: Ecological significance of bacterial enzymes in the marine  
628 environment, in *Enzymes in the environment: activity, ecology, and applications*, edited by R. Burns and R. Dick,  
629 pp. 73–108, Marcel Dekker, Inc., New York., 2002.

630 Horthorn, T., Bretz, F. and Westfall, P.: Simultaneous Inference in General Parametric Models, *Biometrical J.*, 50(3),  
631 346–363, 2008.

632 Ilyina, T., Six, K. D., Segschneider, J., Maier-Reimer, E., Li, H. and Nunez-Riboni, I.: Global ocean biogeochemistry  
633 model HAMOCC : Model architecture and performance as component of the MPI-Earth system model in different  
634 CMIP5 experimental realizations, *J. Adv. Model. earth Syst.*, 5, 1–29, doi:10.1029/2012MS000178, 2013.

635 John Fox and Sanford Weisberg: An {R} Companion to Applied Regression, 2nd ed., SAGE Publications Ltd,  
636 Thousant OAk {CA}., 2011.

637 Kalvelage, T., Jensen, M. M., Contreras, S., Revsbech, N. P., Lam, P., Günter, M., LaRoche, J., Lavik, G. and  
638 Kuypers, M. M. M.: Oxygen sensitivity of anammox and coupled N-cycle processes in oxygen minimum zones,  
639 edited by J. A. Gilbert, *PLoS One*, 6(12), e29299, doi:10.1371/journal.pone.0029299, 2011.

640 Kalvelage, T., Lavik, G., Lam, P., Contreras, S., Arteaga, L., Löscher, C. R., Oschlies, A., Paulmier, A., Stramma, L.  
641 and Kuypers, M. M. M.: Nitrogen cycling driven by organic matter export in the South Pacific oxygen minimum  
642 zone, *Nat. Geosci.*, 6(3), 228–234, doi:10.1038/ngeo1739, 2013.

643 Kalvelage, T., Lavik, G., Jensen, M. M., Revsbech, N. P., Löscher, C., Schunck, H., Desai, D. K., Hauss, H., Kiko,  
644 R., Holtappels, M., LaRoche, J., Schmitz, R. A., Graco, M. I. and Kuypers, M. M. M.: Aerobic microbial respiration  
645 in oceanic oxygen minimum zones, edited by Z.-X. Quan, *PLoS One*, 10(7), e0133526,  
646 doi:10.1371/journal.pone.0133526, 2015.

647 Kämpf, J. and Chapman, P.: *Upwelling Systems of the World*, Springer International Publishing Switzerland, Cham.  
648 [online] Available from: <http://link.springer.com/10.1007/978-3-319-42524-5>, 2016.

649 Kiko, R., Hauss, H., Buchholz, F. and Melzner, F.: Ammonium excretion and oxygen respiration of tropical  
650 copepods and euphausiids exposed to oxygen minimum zone conditions, *Biogeoscience*, 13, 2241–2255,  
651 doi:10.5194/bg-13-2241-2016, 2016.

652 Kirchman, D., K’nees, E. and Hodson, R.: Leucine incorporation and its potential as a measure of protein synthesis  
653 by bacteria in natural aquatic systems., *Appl. Environm. Microbiol.*, 49(3), 599–607, 1985.

654 Kirchman, D. L., Rich, J. H. and Barber, R. T.: Biomass and biomass production of heterotrophic bacteria along

655 140°W in the equatorial Pacific: Effect of temperature on the microbial loop, Deep Sea Res. Part II Top. Stud.  
656 Oceanogr., 42(2–3), 603–619, doi:10.1016/0967-0645(95)00021-H, 1995.

657 Lam, P. and Kuypers, M. M. M.: Microbial nitrogen cycling processes in oxygen minimum zones., Annu. Rev. Mar.  
658 Sci, 3, 317–348, doi:10.1146/annurev-marine-120709-142814, 2011.

659 Lawson, C. E., Wu, S., Bhattacharjee, A. S., Hamilton, J. J., McMahon, K. D., Goel, R. and Noguera, D. R.:  
660 Metabolic network analysis reveals microbial community interactions in anammox granules., Nat. Commun.,  
661 8(15416), 1–12, doi:10.1038/ncomms15416, 2017.

662 Lee, C.: Controls on organic carbon preservation : the use of stratified water bodies to compare intrinsic rates of  
663 decomposition in oxic and anoxic systems., Geochim. Cosmochim. Acta, 56(8), 3323–3335, doi:10.1016/0016-  
664 7037(92)90308-6, 1992.

665 Lindroth, P. and Mopper, K.: High performance liquid chromatographic determination of subpicomole amounts of  
666 amino acids by precolumn fluorescence derivatization with o-phthaldialdehyde., Anal. Chem., 51(11), 1667–1674,  
667 doi:10.1021/ac50047a019, 1979.

668 Llanillo, P. J., Karstensen, J. and Stramma, L.: Physical and biogeochemical forcing of oxygen and nitrate changes  
669 during El Niño / El Viejo and La Niña / La Vieja upper-ocean phases in the tropical eastern South Pacific along 86 °  
670 W, Biogeosciences, 10, 6339–6355, doi:10.5194/bg-10-6339-2013, 2013.

671 Llanillo, P. J., Pelegrí, J. L., Talley, L. D., Pena-Izquierdo, J. and Cordero, R. R.: Oxygen Pathways and Budget for  
672 the Eastern South Pacific Oxygen Minimum Zone, J. Geophys. Res., 123, 1722–1744, doi:10.1002/2017JC013509,  
673 2018.

674 Loginova, A. N., Thomsen, S., Dengler, M., Lüdke, J. and Engel, A.: Diapycnal dissolved organic matter supply into  
675 the upper Peruvian oxycline, Biogeosciences, 16, 2033–2047, doi:10.5194/bg-16-2033-2019, 2019.

676 López-Urrutia, Á. and Morán, X. A. G.: Resource limitation of bacterial production distorts the temperature  
677 dependence of oceanic carbon cycling, Ecology, 88(4), 817–822, doi:10.1890/06-1641, 2007.

678 McDougall, T. J. and Barker, P. M.: Getting started with TEOS-10 and the Gibbs Seawater (GSW) oceanographic  
679 toolbox, SCOR/IAPSO WG 127, , 28, 2011.

680 Van Mooy, B. A. S., Keil, R. G. and Devol, A. H.: Impact of suboxia on sinking particulate organic carbon:  
681 Enhanced carbon flux and preferential degradation of amino acids via denitrification., Geochim. Cosmochim. Acta,  
682 66(3), 457–465, doi:10.1016/S0016-7037(01)00787-6, 2002.

683 Pantoja, S., Rossel, P., Castro, R., Cuevas, L. A., Daneri, G. and Córdova, C.: Microbial degradation rates of small  
684 peptides and amino acids in the oxygen minimum zone of Chilean coastal waters, Deep Sea Res. Part, 56(16), 1055–  
685 1062, doi:10.1016/j.dsr2.2008.09.007, 2009.

686 Paulmier, A. and Ruiz-Pino, D.: Oxygen minimum zones ( OMZs ) in the modern ocean, *Prog. Oceanogr.*, 80(3–4),  
687 113–128, doi:10.1016/j.pocean.2008.08.001, 2009.

688 Piontek, J., Sperling, M., Nöthig, E. M. and Engel, A.: Regulation of bacterioplankton activity in Fram Strait (Arctic  
689 Ocean) during early summer: The role of organic matter supply and temperature., *J. Mar. Syst.*, 132, 83–94,  
690 doi:10.1016/j.jmarsys.2014.01.003, 2014.

691 R Development Core Team: R: A language and environment for statistical computing, [online] Available from:  
692 <http://www.r-project.org>, 2008.

693 Rivkin, R. B. and Legendre, L.: Biogenic carbon cycling in the upper ocean: Effects of microbial respiration,  
694 *Science.*, 291(5512), 2398–2400, doi:10.1126/science.291.5512.2398, 2001.

695 Roullier, F., Berline, L., Guidi, L., Durrieu De Madron, X., Picheral, M., Sciandra, A., Pesant, S. and Stemmann, L.:  
696 Particle size distribution and estimated carbon flux across the Arabian Sea oxygen minimum zone, *Biogeosciences*,  
697 11(16), 4541–4557, doi:10.5194/bg-11-4541-2014, 2014.

698 Schafstall, J., Dengler, M., Brandt, P. and Bange, H.: Tidal-induced mixing and diapycnal nutrient fluxes in the  
699 Mauritanian upwelling region, *J. Geophys. Res.*, 115(C10), C10014, doi:10.1029/2009JC005940, 2010.

700 Schlitzer, R.: Ocean Data View, 2016.

701 Simon, M. and Azam, F.: Protein content and protein synthesis rates of planktonic marine bacteria., *Mar. Ecol. Prog. Ser.*, 51(3), 201–213, 1989.

703 Smith, D. C. and Azam, F.: A simple , economical method for measuring bacterial protein synthesis rates in seawater  
704 using  $^{3}\text{H}$ -leucine, *Mar. Microb. Food Web*, 6(2), 107–114, 1992.

705 Steinfeldt, R., Sültenfuß, J., Dengler, M., Fischer, T. and Rhein, M.: Coastal upwelling off Peru and Mauritania  
706 inferred from helium isotope disequilibrium, *Biogeoscience*, 12, 7519–7533, doi:10.5194/bg-12-7519-2015, 2015.

707 Stramma, L., Schmidtko, S., Levin, L. A. and Johnson, G. C.: Ocean oxygen minima expansions and their biological  
708 impacts, *Deep Sea Res. Part I Oceanogr. Res. Pap.*, 57(4), 587–595, doi:10.1016/j.dsr.2010.01.005, 2010.

709 Strohm, T. O., Griffin, B., Zumft, W. G. and Schink, B.: Growth yields in bacterial denitrification and nitrate  
710 ammonification, *Appl. Environ. Microbiol.*, 73(5), 1420–1424, doi:10.1128/AEM.02508-06, 2007.

711 Sugimura, Y. and Suzuki, Y.: A high-temperature catalytic oxidation method for the determination of non-volatile  
712 dissolved organic carbon in seawater by direct injection of a liquid sample, *Mar. Chem.*, 24(2), 105–131,  
713 doi:10.1016/0304-4203(88)90043-6, 1988.

714 Taylor, G. T., Thunell, R., Varela, R., Benitez-Nelson, C. and Scranton, M. I.: Hydrolytic ectoenzyme activity  
715 associated with suspended and sinking organic particles within the anoxic Cariaco Basin, *Deep Sea Res. I*, 56(8),

716 1266–1283, doi:10.1016/j.dsr.2009.02.006, 2009.

717 Thamdrup, B., Dalsgaard, T. and Revsbech, N. P.: Widespread functional anoxia in the oxygen minimum zone of the  
718 Eastern South Pacific, *Deep Sea Res. Part I Oceanogr. Res. Pap.*, 65, 36–45, doi:10.1016/j.dsr.2012.03.001, 2012.

719 Thrash, C. J., Seitz, K. W., Baker, B. J., Temperton, B., Gillies, L. E., Rabalais, N. N., Henrissat, B. and Mason, U.:  
720 Metabolic roles of uncultivated bacterioplankton lineages in the northern Gulf of Mexico “Dead Zone,” *MBio*, 8(5),  
721 1–20, doi:10.1128/mBio.01017-17, 2017.

722 Tiano, L., Garcia-Robledo, E., Dalsgaard, T., Devol, A. H., Ward, B. B., Ulloa, O., Canfield, D. E. and Peter  
723 Revsbech, N.: Oxygen distribution and aerobic respiration in the north and south eastern tropical Pacific oxygen  
724 minimum zones, *Deep Sea Res. Part I*, 94(October), 173–183, doi:10.1016/j.dsr.2014.10.001, 2014.

725 Ward, B. B.: How nitrogen is lost, *Science.*, 341(6144), 352–353, doi:10.1126/science.1240314, 2013.

726 Weiss, M., Abele, U., Weckesser, J., Welte, W., Schiltz, E. and Schulz, G.: Molecular architecture and electrostatic  
727 properties of a bacterial porin, *Science.*, 254(5038), 1627–1630, doi:10.1126/science.1721242, 1991.

728 Winkler, W. L.: Die Bestimmung des im Wasser gelösten Sauerstoffes., *Berichte der Dtsch. Chem. Gesellschaft*,  
729 21(2), 2843–2854, doi:10.1002/cber.188802102122, 1888.

730

731 **Figure legends**

732

733 **Figure 1:** Station map. All presented stations in the Eastern Tropical South Pacific off Peru sampled in 2017. For detailed  
734 informations about the stations see supplementary Table 1.

735 **Figure 2:** Measured concentrations and calculated proxies for the change of dissolved organic carbon (DOC) and dissolved  
736 oxygen (DO) flux over depth for stations G-T: The average diapycnal diffusivity of mass ( $K_\rho$ ) over depth with confidence interval  
737 and the constant  $K_\rho (1 \times 10^{-3} m^2 s^{-1})$  that was used for further calculations (a). Concentrations of DOC in the upper 100 m and  
738 the resulting change of DOC flux over depth ( $\nabla \Phi$ ) (b). Concentrations of DO in the upper 100 m and the resulting change of DO  
739 flux over depth ( $\nabla \Phi$ ) (c).

740 **Figure 3:** Biotic and abiotic conditions at selected stations exemplary for the sampling conditions. Chlorophyll (a), temperature (b),  
741 total dissolved nitrogen (TDN) (c), dissolved organic carbon (DOC) (d), carbon content of dissolved hydrolysable amino acids  
742 (DHAA) (e) and carbon content of high molecular weight dissolved carbohydrates (DCHO) (f) over depth at different stations from  
743 on- to offshore off Peru.

744 **Figure 4:** Bacterial growth activity at different *in situ* oxygen concentrations from on- to offshore off Peru during April 2017  
745 (M136). Oxygen concentrations (a), total bacterial production (BP) (b), bacterial abundance (c) cell-specific BP (d) over the  
746 upper 800 m depth with a zoom in the upper 100 m (small plots).

747 **Figure 5:** Extracellular enzyme rates at different *in situ* oxygen concentrations during April and June 2017 (M136, M138).  
748 Oxygen concentrations (a), degradation rates of dissolved amino acids (DHAA) by leucine-aminopeptidase (LAPase) (b),  
749 degradation rates of high molecular weight dissolved carbohydrates (DCHO) by  $\beta$ -glucosidase (GLUCase) (c) total potential  
750 LAPase rates ( $V_{max}$ ) (d), Glucase  $V_{max}$  (e), cell abundance (f), cell-specific degradation rates DHAA by LAPase (g), cell-specific  
751 degradation rates of DCHO by GLUCase (h), cell-specific LAPase  $V_{max}$  (i) and cell-specific Glucase  $V_{max}$  (j) at different oxygen  
752 regimes off Peru.

753

754

755

756 **Tables**

757 **Table 1:** Estimates of oxygen and DOC loss over depth based on *in situ* physical observations and bacterial rate measurements. Oxygen and DOC loss rates (mmol m<sup>-3</sup> d<sup>-1</sup>) were  
 758 estimated from the change in oxygen and DOC fluxes over depth. The bacterial uptake of DOC (mmol m<sup>-3</sup> d<sup>-1</sup>) was calculated from bacterial production (mmol m<sup>-3</sup> d<sup>-1</sup>) based on a  
 759 growth efficiency of 10 and 30% (DOC uptake<sub>φ</sub>). The bacterial oxygen demand (BOD, mmol m<sup>-3</sup> d<sup>-1</sup>) and bacterial growth efficiency (BGE<sub>ε</sub>, %) was calculated from bacterial  
 760 production and the assumption that DOC loss can be completely explained by bacterial uptake (BOD<sub>ε</sub>) or estimated based on a BGE of 10 and 30% (BOD<sub>φ</sub>).

761

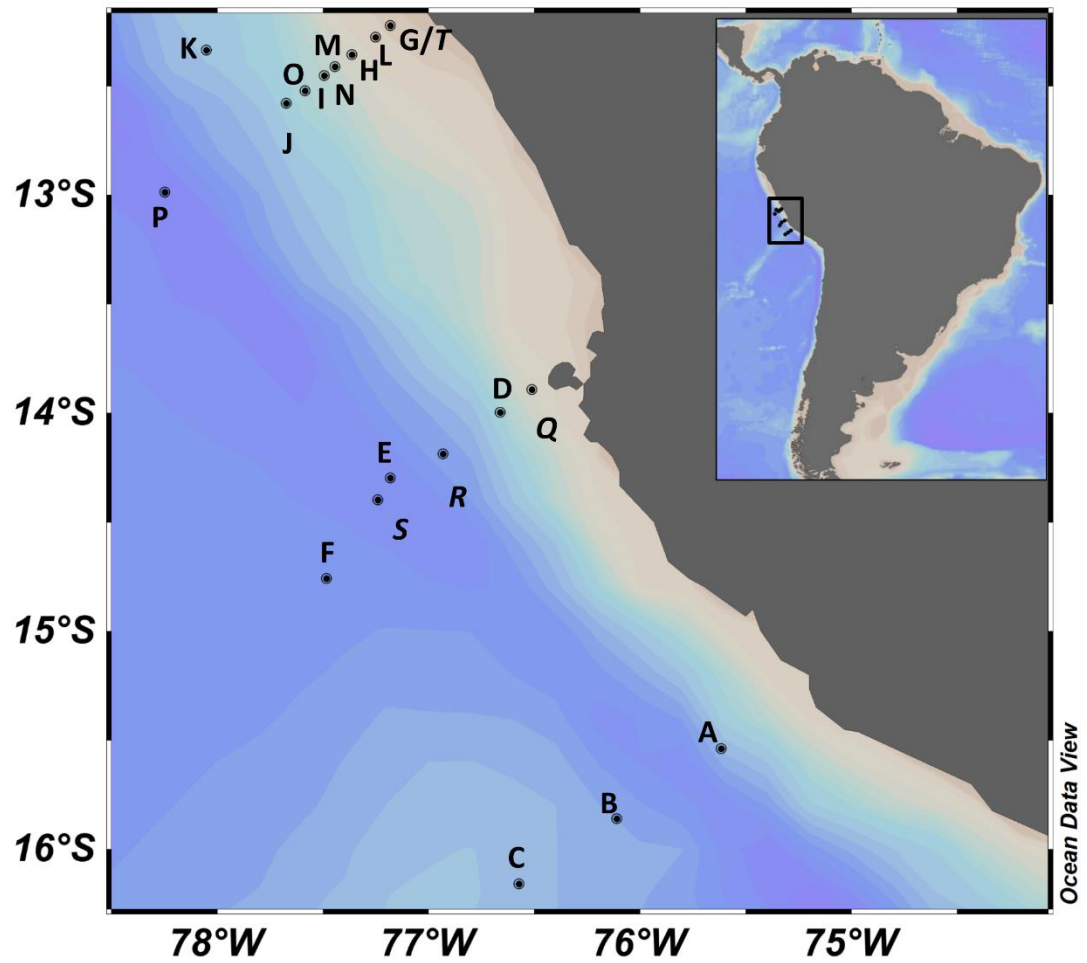
Depth	oxygen loss	DOC loss	DOC uptake <sub>φ10</sub>	DOC uptake <sub>φ30</sub>	Bacterial Production	BOD <sub>ε</sub>	BOD <sub>φ10</sub>	BOD <sub>φ30</sub>	BGE <sub>ε</sub>
	avg	avg	avg min max	avg min max	avg min max	avg min max	avg min max	avg min max	avg min max
MLD-40	10.23	3.4	2.22 0.35 7.10	0.74 0.12 2.37	0.22 0.03 0.71	3.17 2.68 3.36	2.00 0.31 6.39	0.52 0.08 1.66	6.55 1.02 20.92
40-60	5.55	1.13	0.56 0.25 1.46	0.19 0.08 0.49	0.06 0.03 0.15	1.07 0.98 1.10	0.51 0.23 1.32	0.13 0.06 0.34	5.00 2.26 12.97

762

763

764

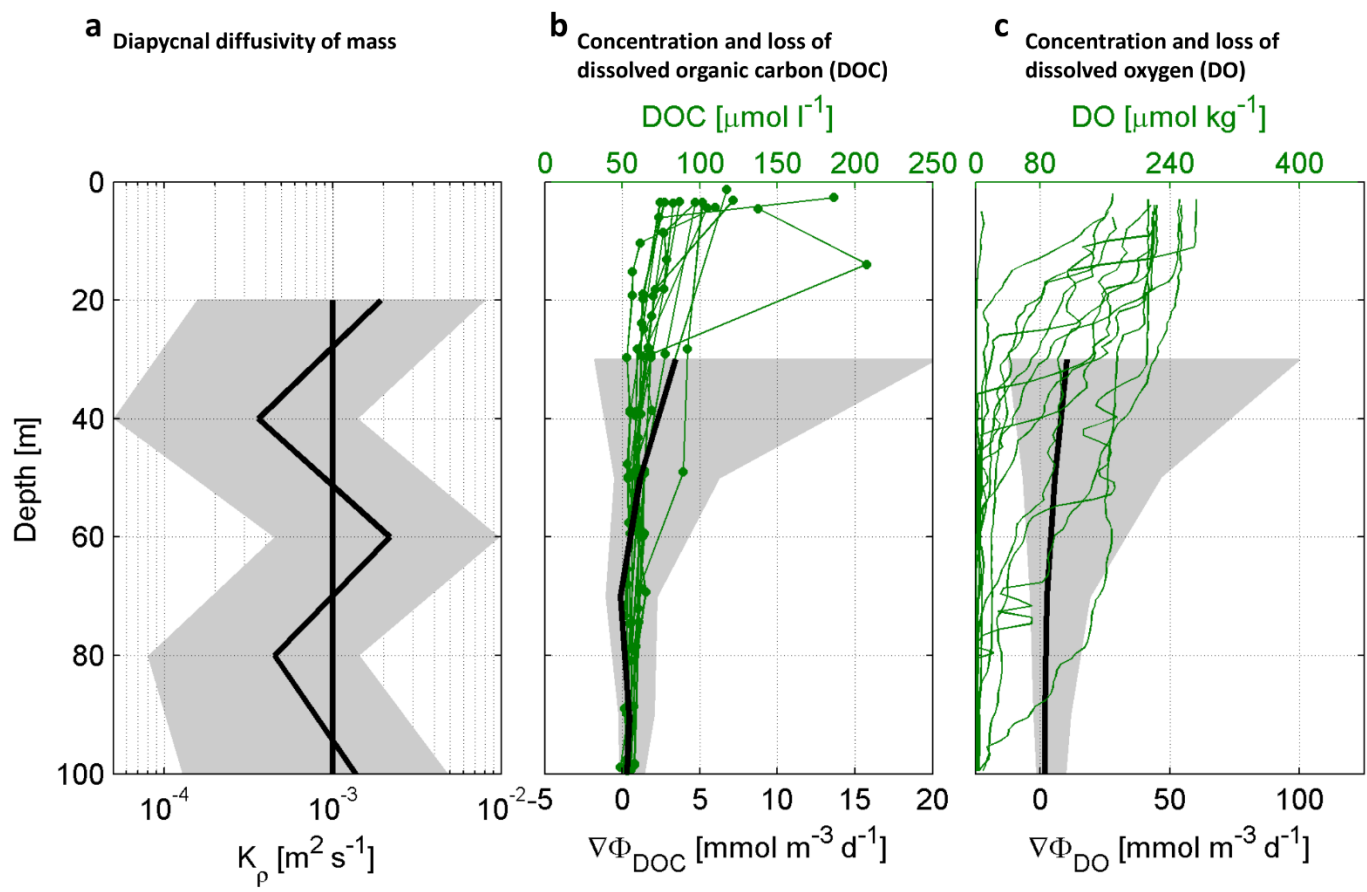
765 **Figures**



766

767 **Figure 1**

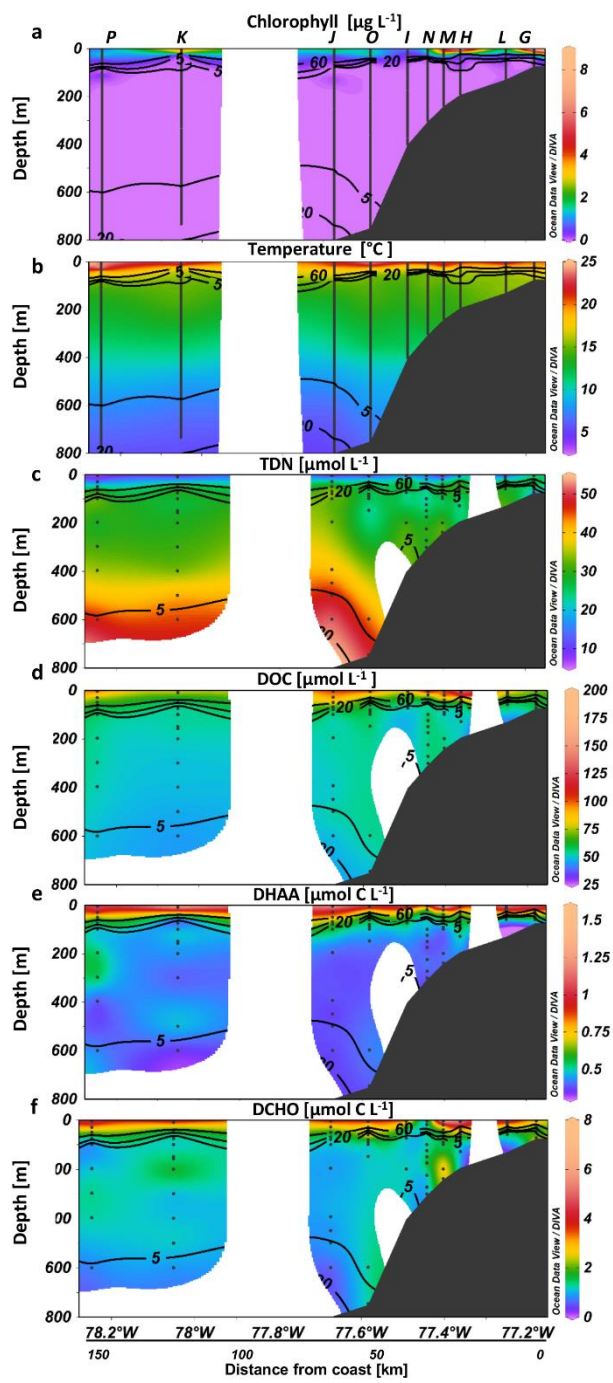
768



769

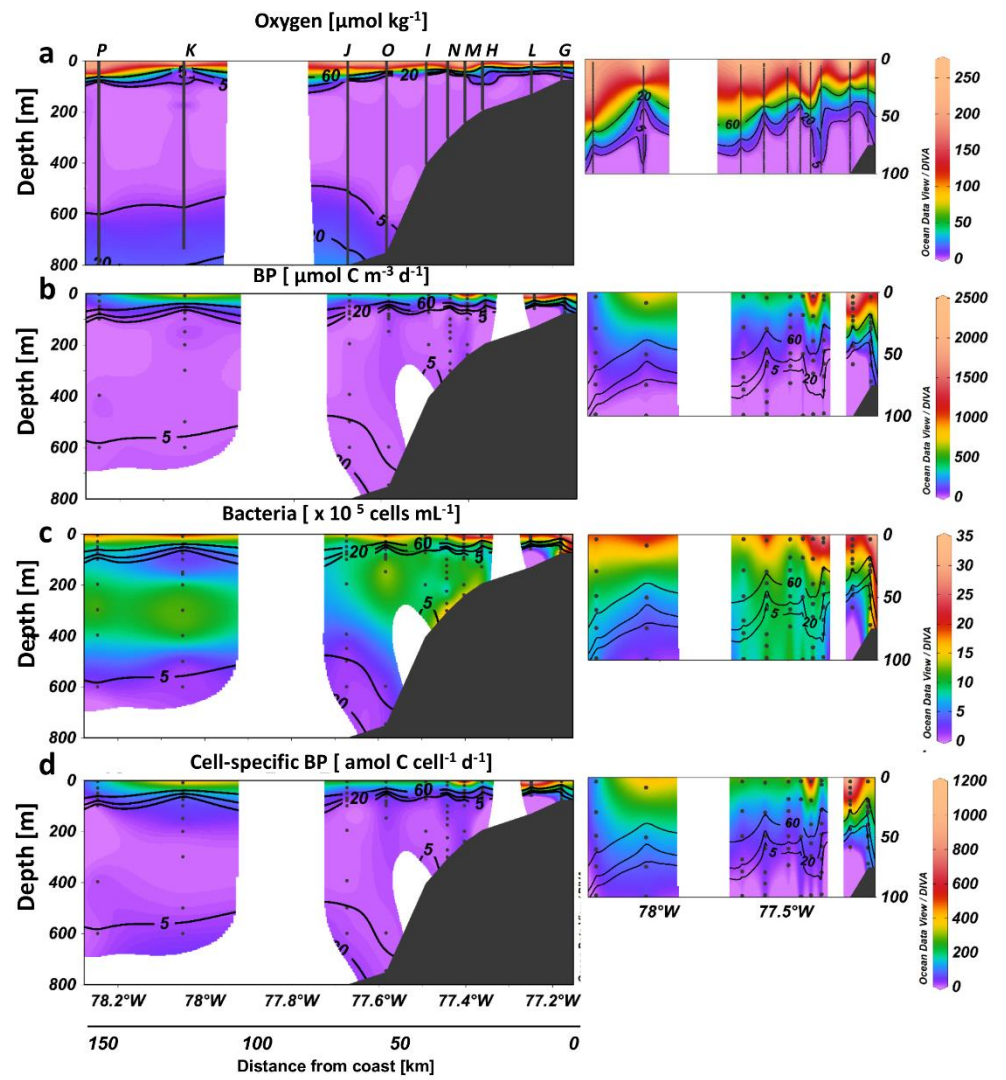
770 **Figure 2**

771

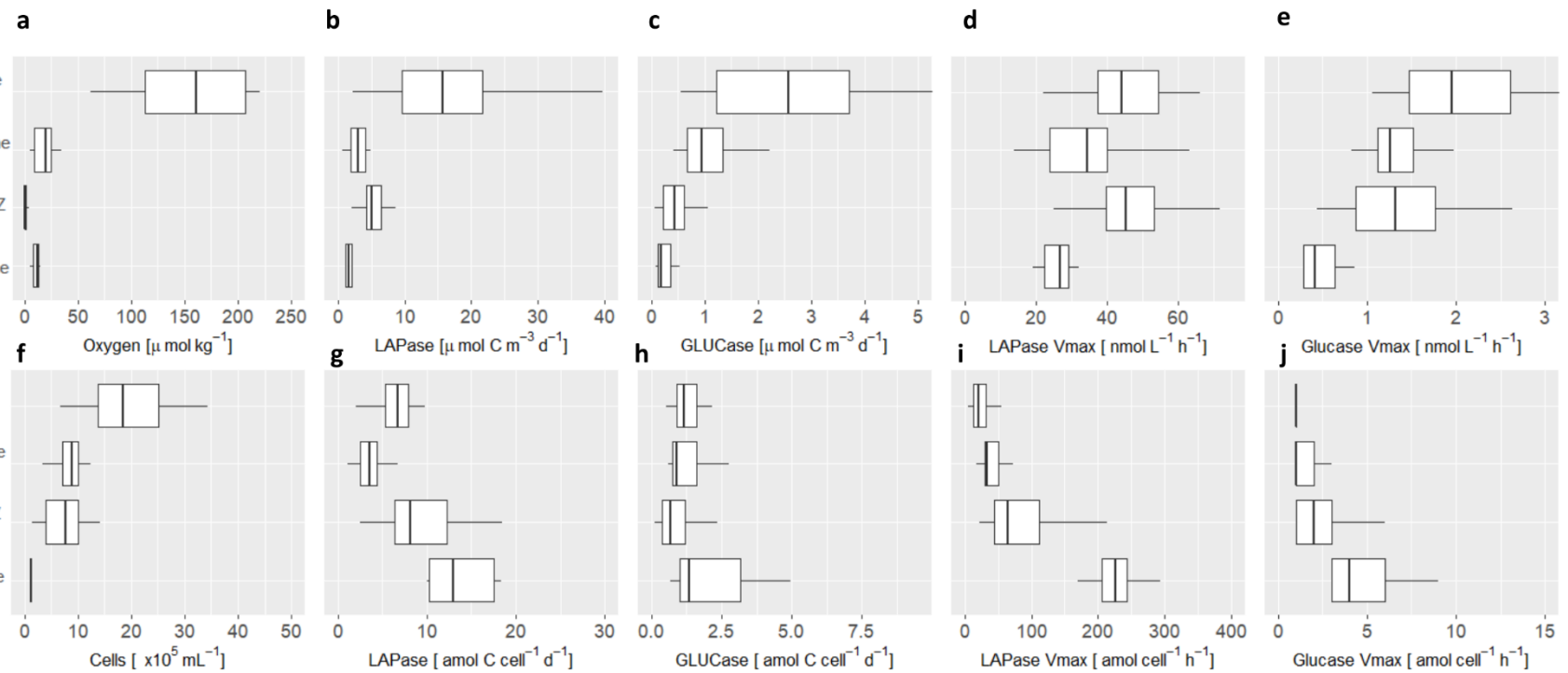


772

773 **Figure 3**



776

777 **Figure 5**

778

779

780

781